Deep-Sea Research I 112 (2016) 137–154

Contents lists available at ScienceDirect

Deep-Sea Research I

journal homepage: www.elsevier.com/locate/dsri

Structure, transport, and vertical coherence of the Gulf Stream from the Straits of Florida to the Southeast Newfoundland Ridge

Christopher S. Meinen [a,*], Douglas S. Luther [b]

[a] Atlantic Oceanographic and Meteorological Laboratory, Miami, FL, United States
[b] University of Hawaii at Manoa, Honolulu, HI, United States

ARTICLE INFO

Article history:
Received 26 May 2015
Received in revised form
5 January 2016
Accepted 6 February 2016
Available online 12 April 2016

ABSTRACT

Data from three independent and extensive field programs in the Straits of Florida, the Mid-Atlantic Bight, and near the Southeast Newfoundland Ridge are reanalyzed and compared with results from other historical studies to highlight the downstream evolution of several characteristics of the Gulf Stream's mean flow and variability. The three locations represent distinct dynamical regimes: a tightly confined jet in a channel; a freely meandering jet; and a topographically controlled jet on a boundary. Despite these differing dynamical regimes, the Gulf Stream in these areas exhibits many similarities. There are also anticipated and important differences, such as the loss of the warm core of the current by 42°N and the decrease in the cross-frontal gradient of potential vorticity as the current flows northward. As the Gulf Stream evolves it undergoes major changes in transport, both in magnitude and structure. The rate of inflow up to 60°W and outflow thereafter are generally uniform, but do exhibit some remarkable short-scale variations. As the Gulf Stream flows northward the vertical coherence of the flow changes, with the Florida Current and North Atlantic Current segments of the Gulf Stream exhibiting distinct upper and deep flows that are incoherent, while in the Mid-Atlantic Bight the Gulf Stream exhibits flows in three layers each of which tends to be incoherent with the other layers at most periods. These coherence characteristics are exhibited in both Eulerian and stream coordinates. The observed lack of vertical coherence indicates that great caution must be exercised in interpreting proxies for Gulf Stream structure and flow from vertically-limited or remote observations.

1. Introduction

As it flows from its origins in the Caribbean/Gulf of Mexico to its end in the high latitudes of the North Atlantic, the Gulf Stream flows through the narrow Straits of Florida (where it is sometimes called the Florida Current), meanders across the Mid-Atlantic Bight, and returns to the coastline on the eastern seaboard of Canada (after which it is called the North Atlantic Current). Along the way it changes from a tightly confined flow through a channel, to a meandering free jet, and finally to a topographically controlled boundary current. As it transits the western North Atlantic, the Gulf Stream widens by a factor of two, deepens by roughly four thousand meters, and increases in transport by nearly a factor of five (e.g., Leaman et al., 1989). Furthermore, as it flows along its course the Gulf Stream is not only the western boundary current of the subtropical North Atlantic gyre but also the pathway for the upper limb of the global meridional overturning circulation (MOC), returning warm surface waters northward towards the subduction regions in the northern reaches of the North Atlantic. Numerous projects have investigated the Gulf Stream all along its length over the past 50 years using a variety of instruments, including moored current meters, inverted echo sounders (IES), pressure-equipped inverted echo sounders (PIES), Lagrangian sub-surface floats and surface drifters, and even submarine cables. Overviews of many of the historical observations of the Gulf Stream structure and transport in the Straits of Florida, Mid-Atlantic Bight, and Southeast Newfoundland Ridge areas can be found in Meinen et al. (2010), Johns et al. (1995), and Schott et al. (2004), respectively.

A recent reanalysis of the data collected as part of the Synoptic Ocean Prediction (SYNOP) experiment in the Gulf Stream near 38°N, 68°W, demonstrated that advances in the analysis of PIES data make possible full-water column four-dimensional estimates of temperature, salinity, density and absolute velocity, yielding a much more detailed picture of the Gulf Stream's structure than had been available previously (Meinen et al., 2009). The same study demonstrated that the inflow to the Gulf Stream from the

* Corresponding author.
E-mail addresses: Christopher.Meinen@noaa.gov (C.S. Meinen), dluther@hawaii.edu (D.S. Luther).

http://dx.doi.org/10.1016/j.dsr.2016.03.002
0967-0637/

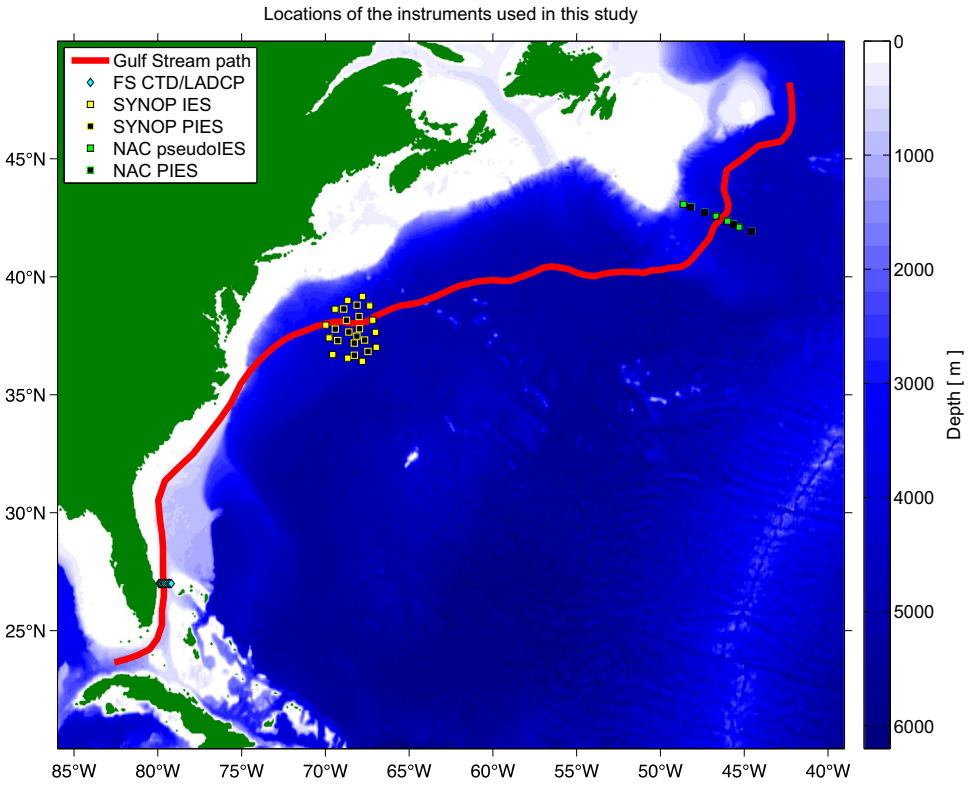

Fig. 1. *Map of the locations of the primary observation sites used in this study. A cartoon/schematic of the Gulf Stream path is also shown, where the path from Cape Hatteras to 50°W is based on the 8-year mean position of the Gulf Stream SST front (Lee and Cornillon, 1996). Bottom topography from Smith and Sandwell (1997) is also shown. Types of observations are noted in the legend.*

neighboring recirculation gyres could be as much as 25% larger than had previously been thought to exist in the SYNOP study area. These results motivated the following two goals of the present paper. First, the four-dimensional temperature, salinity and absolute velocity fields produced by Meinen et al. (2009) from the SYNOP Central Array are used in concert with similar fields from the North Atlantic Current near 42°N (Meinen, 2001) and 55 hydrographic temperature/salinity/velocity sections collected in the Straits of Florida at 27°N (approximately half of which have never been used in previous publications) to highlight the downstream evolution of several important characteristics of the Gulf Stream's mean structure and vertical coherence. These locations are chosen because they represent physically distinctive segments of the Gulf Stream, and because high quality absolute velocity data is available from each location in addition to temperature and salinity data. The second purpose of the paper is to discuss the transport of the Gulf Stream in the context of historical estimates of transport throughout the region to illuminate the flow in these three locations with respect to the diffluent/confluent circulations bounding the Gulf Stream along its path.

2. Data and methods

Measurements from a variety of types of instrument are used herein. Many are common systems, and the details of the original processing and placement of the instruments are left to the papers that are cited. For brevity, only the most critical details of the data sets used are presented in this section.

The primary observations in the Straits of Florida are from 55 shipboard sections using conductivity-temperature-depth (CTD) recorders as well as lowered acoustic Doppler current profilers (LADCP) over the period 2001–2014; nearly half of these sections have not been used in previous analyses. The CTD/LADCP profiles were collected at the nine stations along 27°N indicated in Fig. 1 as part of the NOAA (National Oceanic and Atmospheric Administration) Western Boundary Time Series project (e.g. Szuts and Meinen, 2013; Garcia and Meinen, 2014). For comparison purposes, Pegasus profiler data and current meter mooring data collected during 1982–1984 as part of the Subtropical Atlantic Climate Studies (STACS) program are also discussed (e.g., Molinari et al., 1985a, 1985b; Leaman et al., 1987, 1989; Lee et al., 1985; Johns and Schott, 1987; Lee and Williams, 1988).

The observations used to describe the Gulf Stream where it is a free meandering jet at 68°W were collected as part of the Synoptic Ocean Prediction (SYNOP) experiment. SYNOP involved moored arrays and Lagrangian floats making measurements from Cape Hatteras out to 55°W, spanning an intensive two-year period from 1988 to 1990 (e.g. Pickart and Watts, 1990; Johns et al., 1995; Shay et al., 1995; Watts et al., 1995; Bower and Hogg, 1996). There were three primary arrays of current meter and PIES[1] moorings during the SYNOP experiment: an array just downstream of Cape Hatteras called the Inlet Array, the main array at 68 °W called the Central Array, and an array at 55 °W called the Eastern Array. Like the initial reanalysis of this data set (Meinen et al., 2009), the present study will focus on the data collected in the Central Array (see Fig. 1) due to the wealth of data collected there, utilizing primarily data from the PIES moorings. Data from the 13 tall current meter moorings (e.g. Cronin and Watts, 1996) are employed to verify both that the combination of PIES measured travel times and pressures is capable of reproducing the observed current velocities well and that the vertical coherences for the velocities derived this way, which are available uniformly throughout the water column, are similar to the coherences observed by the sparse set of current meters. It is

[1] Note: Some instruments were simple inverted echo sounders, i.e. without the bottom pressure gauge.

noteworthy that several previous analyses of the PIES data have illustrated that the PIES estimated velocities agree quite well with the direct current meter measurements in these regions, e.g. Fig. 7 of Meinen and Watts (2000) and Fig. 4 of Meinen et al. (2009).

The utility of PIES data is greatly enhanced by the availability of hydrographic data from the region (either simultaneous or historical). For the SYNOP region, conductivity-temperature-depth (CTD) data was acquired from the following sources: 333 CTD profiles from the Anatomy of a Meander project (e.g. Hummon and Rossby, 1998); several transects and ring studies by the University of Rhode Island (e.g. Johns et al., 1989) and the Woods Hole Oceanographic Institution (e.g. Joyce, 1984; Joyce et al., 1986); and the Hydrobase dataset (Lozier et al., 1995). Only CTD profiles that reached at least 1000 dbar and had a near-surface observation within the upper 50 dbar were used. For profiles that lacked values in the upper 10 dbar, the nearest-to-surface temperatures and salinities were copied to the surface assuming a well-mixed layer above 50 dbar.

The observations used at 42°N near the Southeast Newfoundland Ridge come from the North Atlantic Current (NAC) experiment (e.g. Meinen et al., 2000; Meinen and Watts, 2000; Meinen, 2001). This experiment included a line of eight tall current meter moorings and six PIES that were in place for approximately two years during 1993–1995 as a part of a joint program carried out by the Bedford Institute of Oceanography and the University of Rhode Island (see Fig. 1). Due to data losses from several PIES, the temperature and pressure sensors that were on the current meter moorings were combined to create pseudo-IES data and fill the gaps in the PIES line as presented in Meinen and Watts (2000). The shallowest current meters on the tall moorings were determined to have a fatal programming problem such that their data could not be recovered (Watts, personal communication, 1997). As with the SYNOP array, the focus here is on the PIES (including the pseudo-IES records). For the NAC region, 191 CTD profiles were used with the PIES analysis; some profiles were collected during the array deployment and recovery cruises, and others were acquired from the Bedford Institute of Oceanography and the German Hydrographic Service (see Meinen and Watts (2000)).

The fact that the primary data sets used herein all come from different time periods over the past 25 years does not present a significant problem for the interpretation of the analyses herein. Previous work in the Florida Straits (e.g. Meinen et al., 2010), the Mid-Atlantic Bight (e.g. Rossby et al., 2010) and near the Southeast Newfoundland Ridge (e.g. Schott et al., 2004) have compared observations separated by as much as a decade or more in each location and have shown that there is very little interannual variability in the structure and transport of the Gulf Stream at these locations. This does not imply that there have been no long-period variations in the subtropical gyre over the past two and a half decades. Evaluation of the basin-wide Meridional Overturning Circulation at 26.5°N, for example, has found interannual changes of 10–20% (e.g. Smeed et al., 2014; McCarthy et al., 2015). These same studies have indicated, however, that this long-period variability is the result of changes in the basin interior, not the western boundary current. While in some cases the Gulf Stream path may vary at long periods (e.g. in the Mid-Atlantic Bight; e.g. Rossby and Benway, 2000), there is no indication that the mean structure and/or the observed variability at the three locations under study here have significantly varied over the ~25 years spanned by the data at the three locations.

All time series data were smoothed with a second order Butterworth low-pass filter with a 40-h cutoff. The resulting data were then subsampled to once per day (noon GMT). For the bottom pressure records, instrumental drift and tidal variability were estimated and removed prior to low-pass filtering (e.g. Watts et al., 2001a).

2.1. Data processing

The 55 CTD and LADCP sections in the Straits of Florida were processed via standard methods (see, for example, Szuts and Meinen (2013) and Garcia and Meinen (2014)). Details on the Pegasus and current meter processing during STACS can be found in Leaman et al. (1987) and Lee and Williams (1988) and references therein.

The IES and PIES datasets at both 38°N and 42°N have been previously processed (Meinen et al. (2009) and Meinen and Watts (2000), respectively). The derived profiles of velocity and hydrographic variables are used herein, with modifications and/or augmentations where noted. The methods used are reviewed here briefly for those unfamiliar with these instruments. The Inverted Echo Sounder (IES) and the Pressure-equipped Inverted Echo Sounder (PIES) have been in use for many years (e.g. Rossby, 1969; Watts and Rossby, 1977; Meinen and Watts, 1998; Donohue et al., 2010). The utility of these instruments was greatly enhanced by the development of the Gravest Empirical Mode (GEM) technique that takes advantage of the known vertical structural characteristics of the water properties of a particular oceanic region as revealed by hydrographic profiles (e.g. Meinen and Watts, 2000; Watts et al., 2001b). An example GEM lookup table for temperature for the North Atlantic Current region is shown in Fig. 2 to illustrate both the resolution and the typical accuracy of the GEM method; similar lookup tables can be derived for salinity and density (not shown).[2] GEM-derived time series of full-water-column density profiles at each IES/PIES site can be vertically integrated to yield dynamic height anomaly time series. Subsequently, dynamic heights from neighboring sites can be horizontally differenced to give full-depth profiles of geostrophic velocity relative to an assumed level of no motion. When an absolute geostrophic reference velocity is available, such as the bottom velocity variations that can be determined by differencing the PIES bottom pressure measurements, time series of absolute velocity profiles are determined (e.g. Meinen and Watts, 2000). Meinen et al. (2009) presented the details of how the SYNOP IES and PIES data were combined to provide four-dimensional estimates (Longitude, Latitude, Pressure, and Time) of temperature, salinity, density, and absolute velocity. The details of the original analysis of the NAC PIES can be found in Meinen and Watts (2000) and Meinen (2001). Note that because the NAC experiment involved only a single line of moored instruments, only the component of the velocity perpendicular to the array was determined by the line of PIES. In SYNOP, where there were multiple lines of moorings (see Fig. 1), both horizontal components of velocity were determined.

The moored current meter velocity and pressure data from 7 tall current meter moorings in the NAC array and 13 tall current meter moorings in the SYNOP Central Array that were collocated with the PIES (except for one mooring set only during the second year of the experiment without a PIES near its base) are employed herein. Each of the SYNOP moorings had instruments at nominal depths of 400, 700, 1000, and 3500 dbar. During the NAC experiment, up to seven levels of instruments were distributed between 400 dbar below the sea surface to 100 dbar above the bottom.[3] In SYNOP, the individual current meter moorings exhibited pressure deflections (blow-over) with root-mean-squared values

[2] Note that in the original analysis of the NAC study (Meinen and Watts, 2000), wherein the GEM technique was first developed, no salinity GEM field was shown or used in the analysis. This field was created at the time of the original study but was not included in the calculations or publication.

[3] The 400 dbar level current meters in the NAC experiment had an unrecoverable programming error that prevented the velocity data from being useful (Watts, personal communication, 1997).

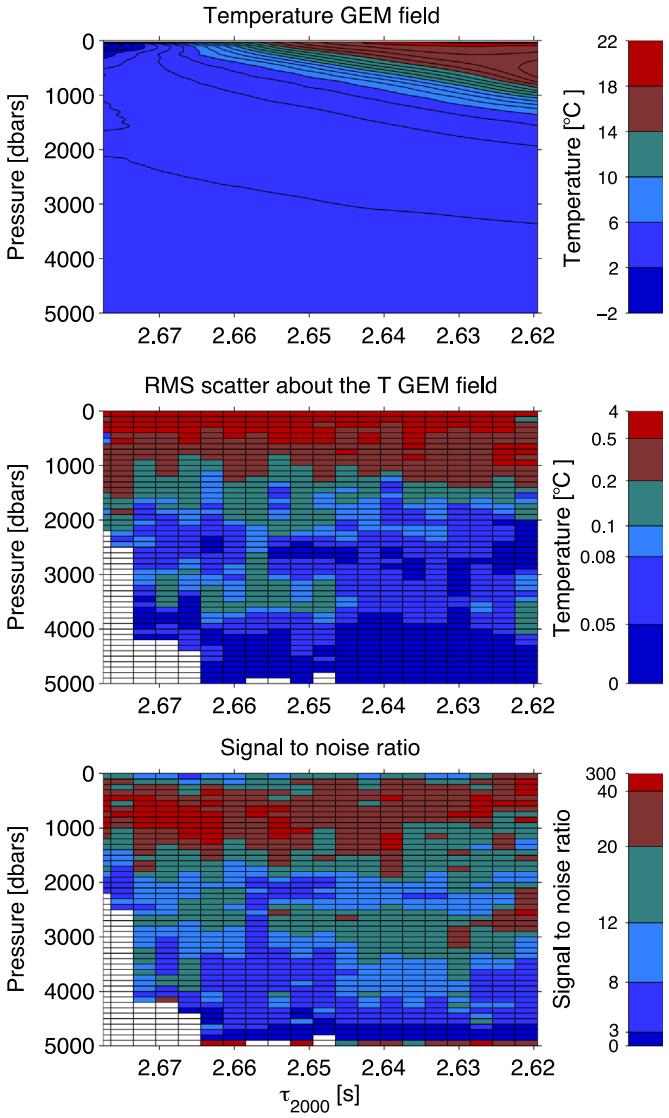

Fig. 2. *Example of a temperature lookup table for GEM analysis of IES data developed using CTD data from the NAC region. Top panel – GEM lookup table of temperature; middle panel – root mean squared (RMS) scatter between the original CTD measured temperatures and the lookup table values; bottom panel – signal to noise ratio based on the observed RMS scatter. See Meinen et al. (2009) for more information on how the RMS and signal-to-noise values are calculated.*

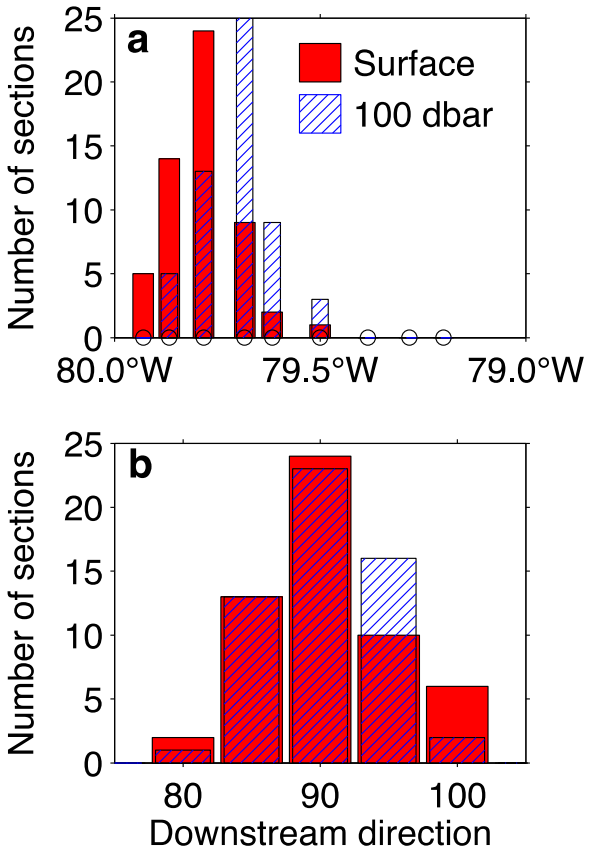

Fig. 3. *a) Histogram of the longitude of the peak velocity observed at the surface (red solid) and at 100 dbar (blue cross-hatch) from the 55 CTD/LADCP sections collected at 27°N. Locations of the nine stations are indicated by circles on lower axis. b) Histogram of the direction of the flow at the location of the peak velocity at the surface or 100 dbar; direction measured in degrees counter-clockwise from East, so 90° is northward. (For interpretation of the references to color in this figure legend, the reader is referred to the web version of this article.)*

of 75–150 m, with a peak deflection of approximately 600 dbar. Cronin and Watts (1996) used temperature and pressure measurements from collocated sensors on the current meter moorings to estimate corrections for this mooring motion. For the NAC current meters, no mooring motion correction was applied. As noted earlier, the current meter mooring data are used primarily to illustrate both that the determination of shear profiles from IES measured travel times, combined with reference velocities derived from bottom pressure, is capable of reproducing the observed current meter signals well (see also Fig. 7 of Meinen and Watts (2000)), and that the subsequent vertical coherences of horizontal currents estimated by each technique are similar.

2.2. Stream coordinates analysis

Previous investigations of the Gulf Stream and other major currents have demonstrated that the estimated mean structures of horizontal currents and water properties depend strongly on the averaging technique applied, which can result in significant differences in dynamical interpretation (e.g. Johns et al., 1995; Bower and Hogg, 1996; Meinen et al., 2009). For example, averages made in an Eulerian coordinate system yield much weaker horizontal gradients than averages made in "stream" coordinates. Stream coordinates are a common analysis technique wherein observations are averaged in distance bins determined relative to some unique characteristic of a meandering current rather than as a function of geographic location (e.g. Johns et al., 1995; Meinen and Luther, 2003). The SYNOP and NAC data were both analyzed previously in stream coordinates (see Meinen et al. (2009) and Meinen (2001), respectively, and citations therein); the origins and stream orientations used for the stream coordinates systems are determined from the positions where the 12 °C isotherm crosses 500 dbar for the SYNOP data, and where the 10 °C isotherm crosses 450 dbar for the NAC data. In the Straits of Florida there is little room for the Florida Current/Gulf Stream to meander, as is illustrated by histograms of the cross-channel location of the peak velocity (Fig. 3a) and of the direction of the peak velocity from the CTD/LADCP sections (Fig. 3b). Given the minimal meandering (generally less than ± 0.2ºof longitude, or less than ± 20 km) and minimal turning of the peak velocity core (generally less than ± 5°), a stream coordinates analysis was considered unnecessary for the flow through the Straits of Florida. Eulerian averaging essentially produces a stream coordinates mean at this location.

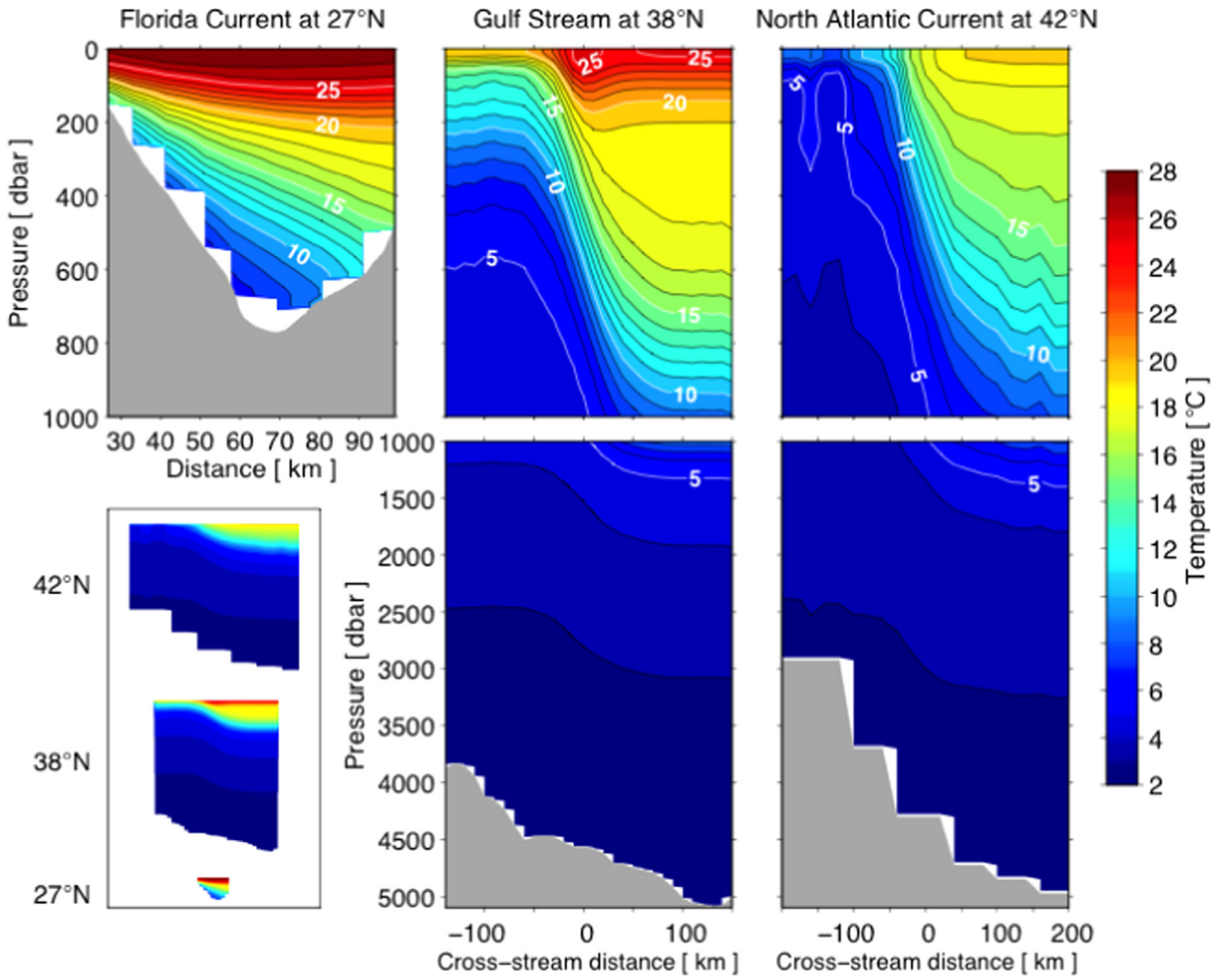

Fig. 4. *Mean temperature sections at three locations along the path of the Gulf Stream. Upper left: Eulerian mean in the Straits of Florida at 27°N. Center: Stream coordinates mean at 38°N, 68°W. Right: Stream coordinates mean at 42°N just downstream of the Southeast Newfoundland Ridge. Note the different horizontal scales of the three sections and the condensed vertical scale of the deeper portions of the 38°N and 42°N sections. Gray shading denotes the ocean bottom in all panels, where bottom depths have been averaged based on the contributions of observation sites for the stream coordinates sections. Contour interval is 1 °C, with every fifth contour displayed in white and labeled. The small inset panel at lower left shows the sections at consistent horizontal and vertical scales.*

3. Results

3.1. Downstream evolution of the structure of the Gulf Stream

Consistent with expectations from previous research, as the Gulf Stream flows from the Straits of Florida to the Mid-Atlantic Bight to the Southeast Newfoundland Ridge the core of the current cools while the thermocline depth change across the front remains nearly constant at around 700–1000 dbar total (Fig. 4). Only in the Mid-Atlantic Bight is a strong mode water layer evident at pressures of 200–500 dbar offshore of the core (Fig. 4), consistent with this area being within the source region for 18 °C Subtropical Mode Water (e.g. Worthington, 1959; Ebbesmeyer and Lindstrom, 1986). The cooling of the core of the current continues downstream, with the peak temperature dropping from 27 °C at 27°N to 25 °C at 38°N to 19 °C at 42°N, and by 42°N there is no longer a recognizable warm temperature core at the center of the current (Fig. 4). The subsurface peak salinity core in horizontal sections across the current exists at both 27°N and 38°N (36.7 psu at 200 dbar), but it has essentially disappeared by the time the current reaches 42°N (Fig. 5). The strength of the salinity gradient across the front, however, strengthens as the Gulf Stream flows north, increasing from about 1.1 psu across 100 km at 38°N to about 1.7 psu across 100 km at 42°N (estimated between 100 and 200 dbar below the surface). The increase at 42°N is due to the influence of the cold, fresh Labrador Current flowing southward and retroflecting to flow northward along the inshore edge of the Gulf Stream/North Atlantic Current north of the Southeast Newfoundland Ridge (e.g. Rossby, 1996; Schott et al., 2004).

The along-stream velocity structure of the current has both important similarities and important differences as it flows downstream (Fig. 6). At all three locations, the expected offshore shift of the velocity core with increasing depth is obvious (e.g. Leaman et al., 1989; Johns et al., 1995). The highest mean surface velocity (178 cm s^{-1}) is found at 27°N where the current is narrowest, with the peak velocity dropping to 170 cm s^{-1} at 38°N and 90 cm s^{-1} at 42°N.[4] The Gulf Stream broadens, with a width between zero velocity contours of about 80 km in the Straits of

[4] The velocities reported here for 38°N and 42°N are geostrophic averages between PIES sites roughly 40 km apart, while the LADCP velocities at 27°N are direct point measurements in a horizontal sense. Comparison of stream coordinates averaged direct measurements to geostrophic measurements reveals that the latter can reflect numbers as much as 10% lower due primarily to the horizontal smoothing associated with the geostrophic method (e.g. Johns et al., 1995; Meinen et al., 2009).

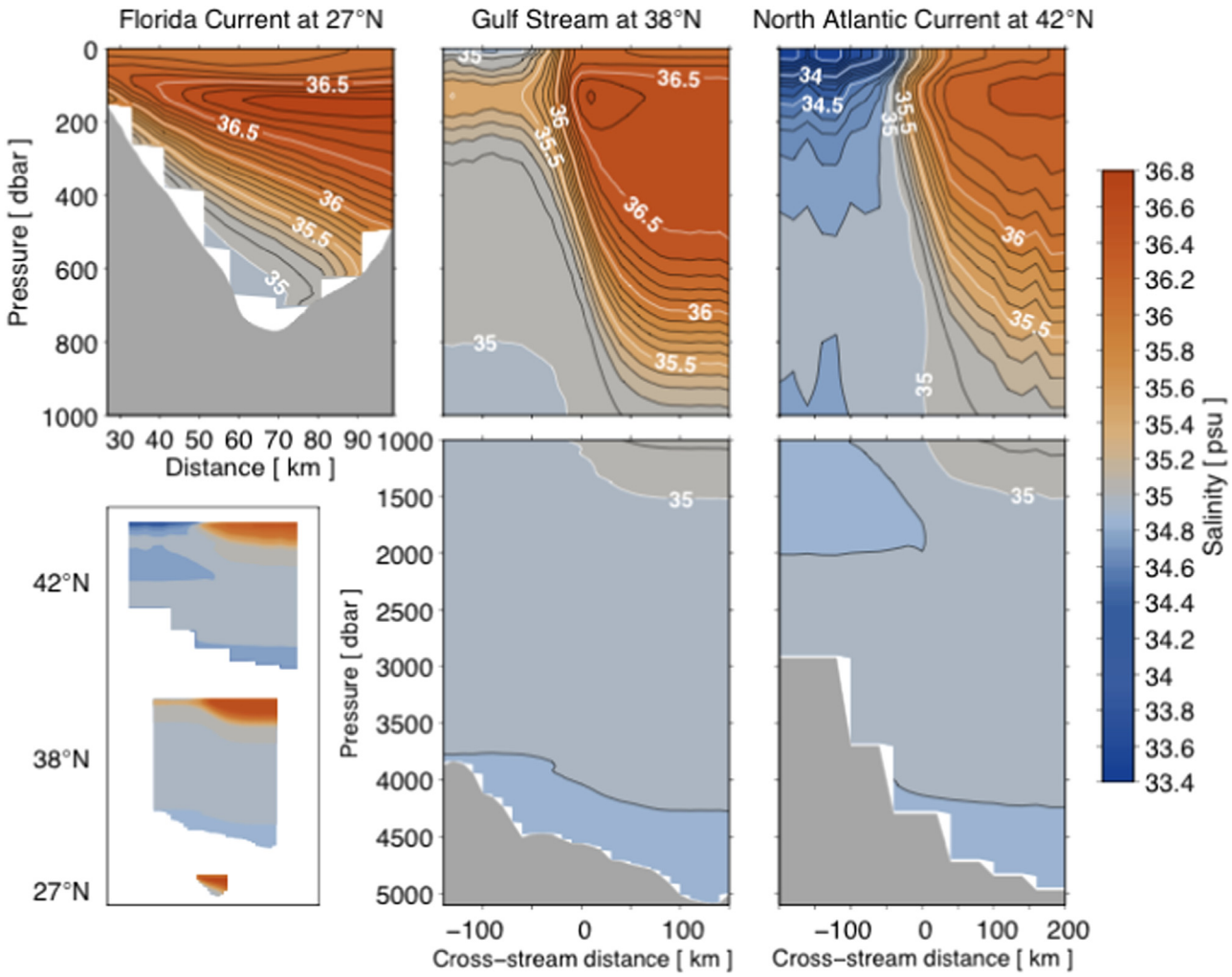

Fig. 5. *Same as Fig. 4 but showing salinity rather than temperature. Contour interval is 0.1 psu, with every fifth contour displayed in white and labeled.*

Florida at 27°N, about 230 km at 38°N, and about 280 km at 42°N. At all three locations the Gulf Stream is clearly reaching to the bottom in a time-mean sense despite the significant increase in depth between 27°N and 38°N. The deep velocities at 42°N are slightly larger than those at 38°N, perhaps reflecting the influence of the Mann Eddy at 42°N (Mann, 1967; Rossby, 1996). Temporal change between the SYNOP (1988–1990) and NAC (1993–1995) experiments is a reasonable hypothesis for this difference; however, comparison between the NAC observations in 1993–1995 and observations collected in 1991–2001 at precisely the same locations (Schott et al., 2004) indicates little change in the deep flows over time.

The cross-stream velocity gradients, as well as the sharpness of the upper pycnocline, clearly decrease as the Gulf Stream moves northward, with peak potential vorticity values at 38°N exceeding those at 42°N by roughly a factor of two, and those at 27°N exceeding those at 38°N similarly (Fig. 7). Potential vorticity (PV; e.g., Gill, 1982) is calculated in a standard manner via

$$PV = \rho^{-1}\,\delta\sigma_\theta/\delta z(f+\zeta)$$

where ρ, σ_θ, f, and ζ are the density, potential density, Coriolis parameter, and the vertical component of the relative vorticity, respectively. Relative vorticity at 27°N and 42°N is approximated as the cross-stream gradient of along-stream velocity because that is the only component that can be calculated with the data available. Meinen et al. (2009) have shown that the along-stream gradient of cross-stream velocity can be significant at 38°N (> 10% of the Coriolis parameter; Fig. 8 shows the two relative vorticity components as recalculated here). This term has been included in the PV calculation at 38°N shown in Fig. 7; however, the conclusions drawn here are not significantly altered if this term is neglected. At 27°N there is no obvious vertical layer where the cross-front gradient in PV is small (Fig. 7), suggesting that horizontal exchange across the front in the tightly confined Straits of Florida is small at all depths. By the time the Gulf Stream reaches 38°N the cross-frontal gradient in PV is very weak at pressures deeper than 300–400 dbar, and by 42°N the cross-frontal gradient in PV has weakened even further below 200 dbar, suggesting that the "blending" of waters across the front is quite possible, consistent with previous work (e.g. Bower et al., 1985; Logoutov et al., 2001). Below 1500 dbar at both 38° and 42°N there is essentially no cross-stream gradient in PV, with the noisy contour levels being nearly horizontal, indicating uninhibited mixing across the Gulf Stream is possible at these depths.

3.2. *Vertical coherence of the flow of the Gulf Stream*

Historical study of the Gulf Stream (and other prominent oceanic currents) began with studies of the near surface conditions, which were all that the observational systems of the times could reach. It was often assumed either that there was no flow at depth or that the deep motion was highly correlated with the surface flow (e.g. Hogg, 1992). This latter idea is formalized in the concept of 'equivalent barotropic' flow that many use to

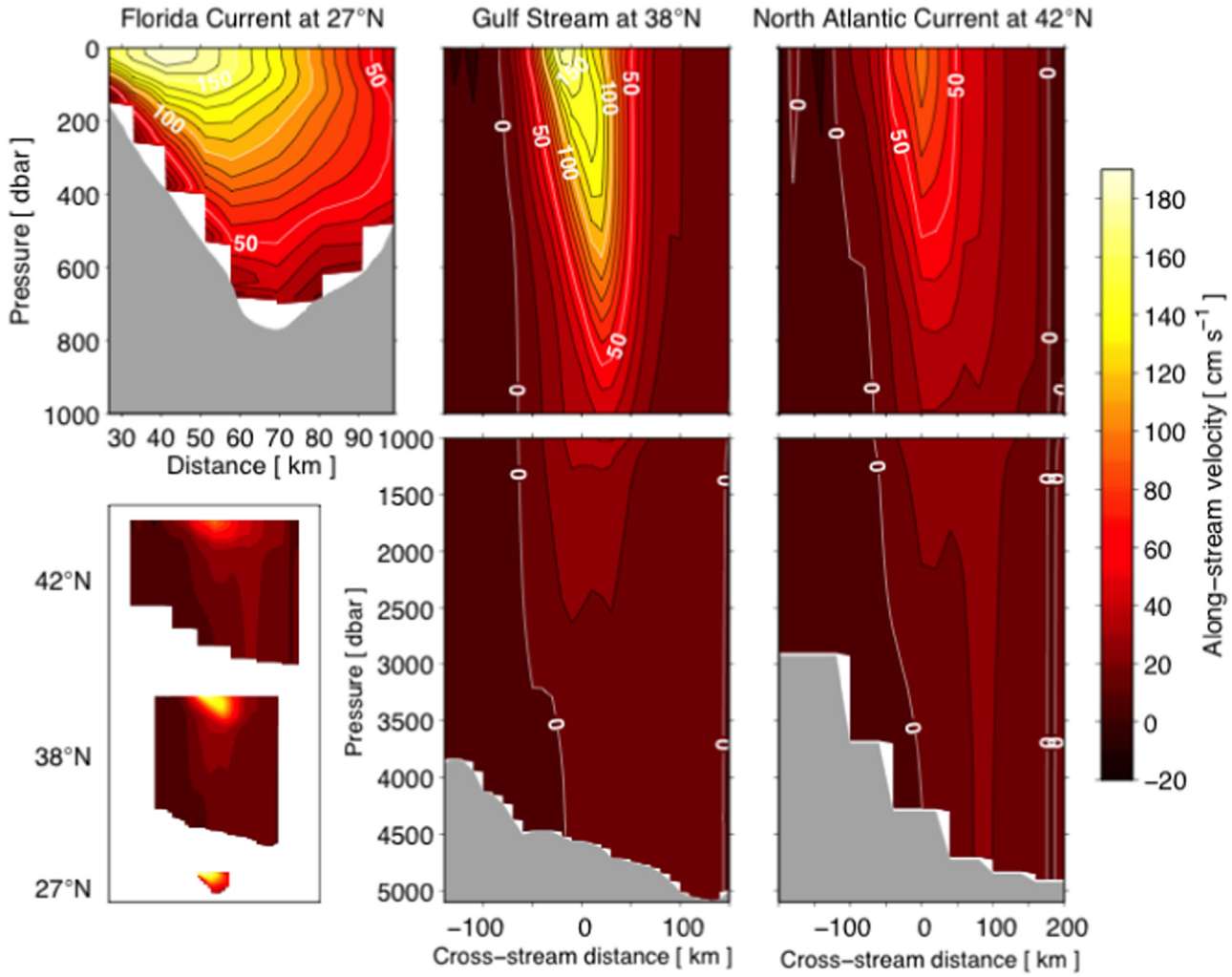

Fig. 6. *Same as Fig. 4 but for along-stream velocity rather than temperature. For the LADCP velocity estimates in the Straits of Florida the northward component is shown. At 42°N, the velocity shown is the component of the velocity perpendicular to the section shown in Fig. 1, as discussed in the text. At 27°N and 42°N the Gulf Stream exhibits only limited direction changes. Contour interval is 10 cm s^{-1}, with every fifth contour displayed in white and labeled.*

characterize the flow of the Gulf Stream itself (e.g., Schmeits and Dijkstra, 2000). These assumptions tended to arise due simply to a lack of data from the deep ocean, and perhaps due to the hope that surface observations can be used to explain what is going on at depth.

Recently, the vertical coherences of the Kuroshio Extension currents have been estimated using moored instruments (Greene et al., 2012), and in the Gulf Stream the vertical correlation of currents in the upper 700 m has been estimated from weekly shipborne ADCP transects between Bermuda and New Jersey (Rossby et al., 2010). The data sets reanalyzed herein provide an opportunity to test exactly to what extent the deep flows are coherent with the surface flows, and at what time scales. This discussion will initially focus on the data from the SYNOP Central array because it provides both the meridional and zonal components of the velocity, whereas the Straits of Florida and NAC observations provide only the along-stream component of the velocity.

Correlation and coherence in the vertical dimension in the ocean are often thought of in terms of the vertical normal modes (e.g. Gill, 1982); however, the basic normal mode decomposition posits a single vertical profile of the buoyancy frequency (N^2), which is not appropriate near strong currents where the vertical density profile changes significantly across the front (e.g., see Fig. 4, imagining temperature as a rough proxy for density). This study will instead calculate vertical coherence strictly empirically, identifying one particular level and then determining the coherence of the flow at all other levels relative to that initial chosen level. The Appendix provides a discussion that should allay concerns regarding the use of PIES-GEM velocities for the calculation of coherence independently at different levels – note also that as mentioned earlier, previous work has demonstrated that the PIES-GEM velocities reproduce well those measured by direct current meters, e.g. Fig. 7 of Meinen and Watts (2000) and Fig. 4 of Meinen et al. (2009); see also Fig. A2 in the Appendix herein. The coherences presented here, calculated via the Welch's averaged periodogram method, are determined for time scales between 10 days, a reasonable lower-bound given the 40-hour low-pass filtering applied, and 365 days, the maximum possible time scale reasonably discernible in a two-year record. Coherences are calculated using a 380-day window for each time series, with a 50% overlap. It is fairly commonplace to see both coherence amplitude and the square of the coherence amplitude referred to as 'coherence' in the literature; for clarity, note that coherence values presented herein are all coherence squared. Where possible, Eulerian-coordinate data from multiple sites within the array are used to increase the number of observations (appropriately averaging coherence and/or spectra) in order to improve statistical reliability.

Examining the coherence between the surface velocity and deeper levels in Eulerian coordinates from 13 sites within the

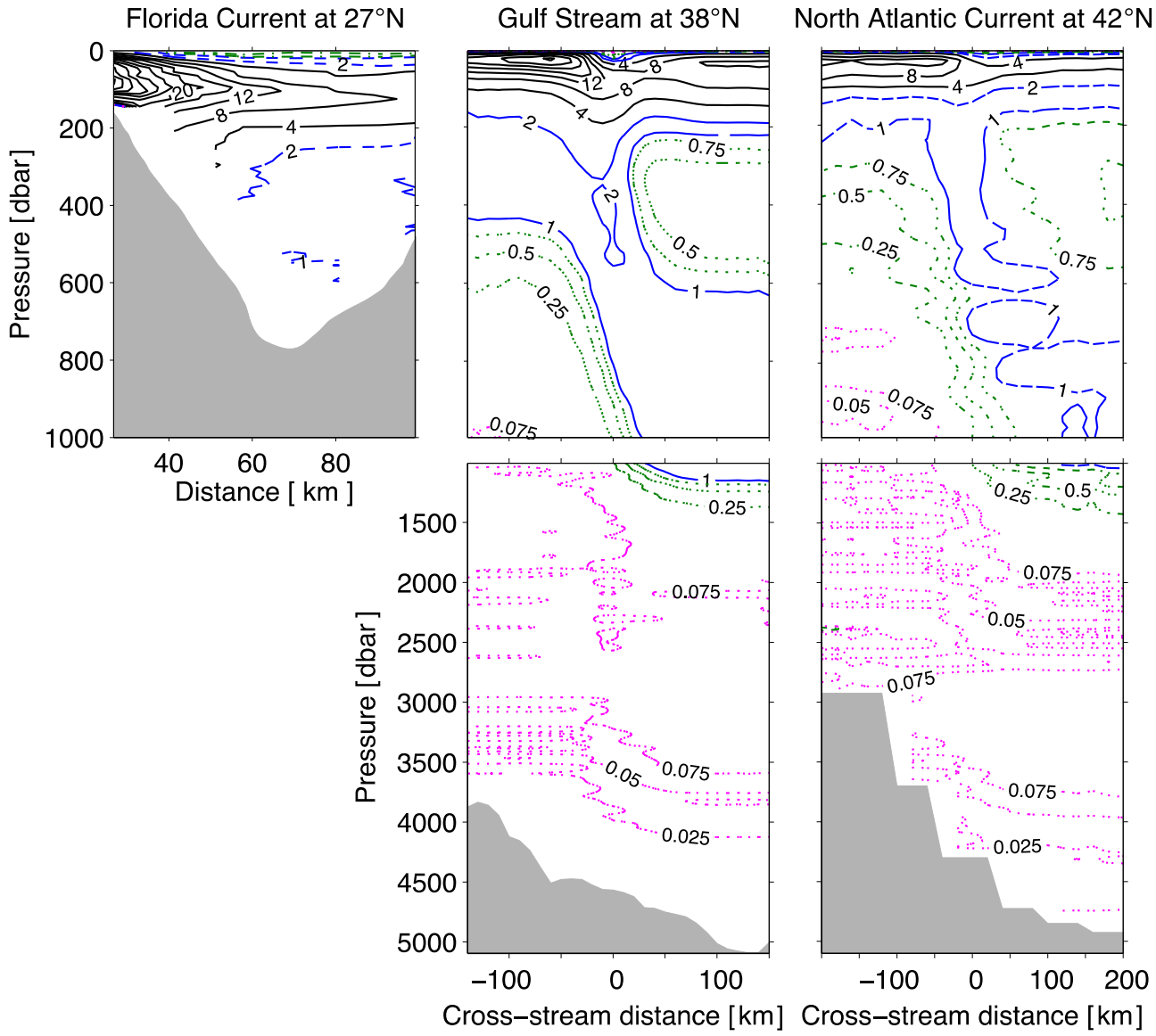

Fig. 7. *Similar to Fig. 4 but for potential vorticity rather than temperature. Potential vorticity is calculated as discussed in the text (units: 10^{-10} m^{-1} s^{-1}). Four contour levels are used in this figure to illustrate the signals at different depths: Solid black contours are for intervals of 4; Solid blue contours are for intervals of 1; Dash-dot green contours are for intervals of 0.25; and Dotted magenta contours are for intervals of 0.025. Below ~1500 dbar the values become very small and are dominated by noise – the patterns are not clear. (For interpretation of the references to color in this figure legend, the reader is referred to the web version of this article.)*

array (Fig. 9) shows that only at periods smaller than about 50 days is there any statistically significant (from zero) coherence between the geostrophic velocities near the surface and velocities at pressures greater than 200–300 dbar (keeping in mind that the PIES-GEM data will include only the geostrophic components of the flow, neglecting Ekman, cyclostrophic, etc.). The high coherence through the upper 200–300 dbar and weak or insignificant coherence below is somewhat similar to the correlation patterns that have been observed slightly further west near 70°W in the weekly repeat shipboard acoustic Doppler current profiler (ADCP) sections collected by the Oleander project (Rossby et al., 2010). The Oleander ADCP data, however, show a decrease in correlation from the surface down to 500 m and then a noticeable increase in correlation below 500 m, whereas in the data presented here there is no indication of increasing coherence between the surface velocity and velocities below 500 dbar at any time scale. The increase in correlation below 500 m that is found in the Oleander data is observed in a single depth bin at 600 m that is the deepest depth consistently observed in their ADCP data, so it may prove to be an artifact, although they indicate it shows a statistically significant correlation at the 95% level (Rossby et al., 2010). The associated phases determined from the coherence calculations here (not shown) are very small, generally less than 5–10° (or π/36–π/18 radians). Even for the meridional velocity at periods of 30–50 days, where the statistically significant coherence extends over the largest vertical range, the coherence phases do not exceed 20°. Greene et al. (2012) found much larger phase lags in the Kuroshio Extension, up to 90°, which may indicate a difference in the vertical interactions in the Kuroshio versus the Gulf Stream. The very small lags found in the Gulf Stream suggest little indication of vertical propagation at this location, at least for the time scales observable with these data. As the calculated phase lags are all quite small, further discussion of the lags will be curtailed.

In the data presented herein there are stronger coherences deeper than 500 dbar in the meridional velocities than in the zonal velocities or the total speed at periods shorter than 50 days, which may reflect the importance of meridional motions

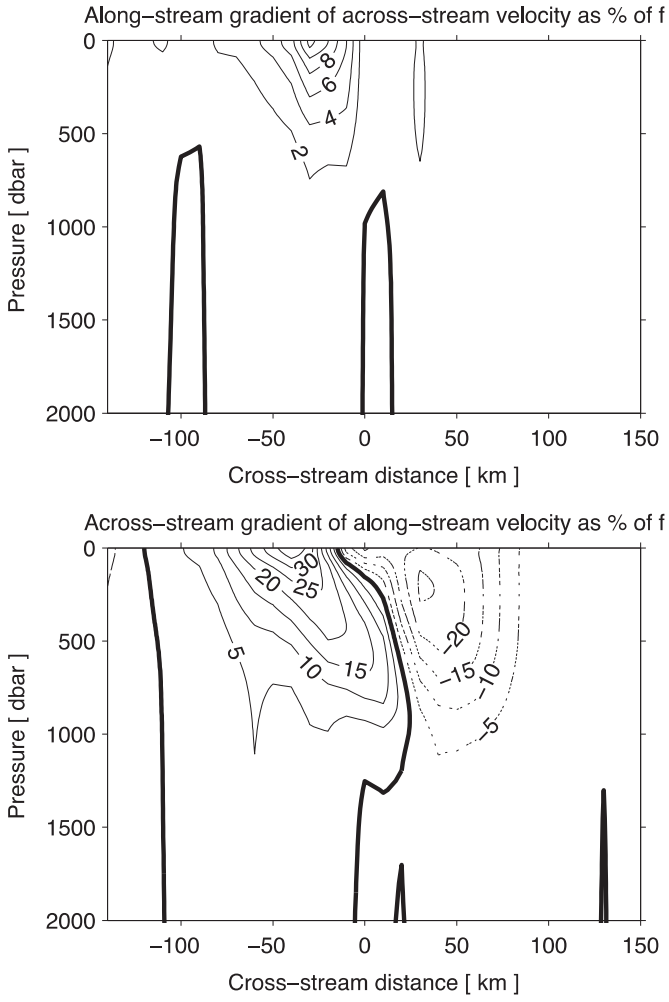

Fig. 8. *Comparison of the relative vorticity terms to the magnitude of the Coriolis parameter f at 38°N. Top: The along-stream gradient of across-stream velocity. Bottom: The across-stream gradient of along-stream velocity. Values are reported as percentages of the Coriolis parameter. Dotted contours indicate negative values. Note the different contour intervals in the two panels.*

associated with the meandering and interaction with deep cyclones found previously in this region (e.g. Savidge and Bane, 1999a, 1999b). The variance-preserving spectra of the velocities (lower panels in Fig. 9) suggest that the extended vertical range of horizontal coherence near 30–50 days is associated with a time scale where significant energy is observed both at the surface and at 500 dbar. At longer periods than 50 days there is no apparent connection between velocity variability at the surface and deeper flow even within the main thermocline depth layer, despite significant energy at these time scales. It is possible that longer datasets might reveal a weakly significant coherence between the surface and the main thermocline in these longer time scales. As noted earlier, the higher vertical coherence at periods of 30–50 days likely reflects the occasional development and propagation of meanders, and the interaction and dynamical coupling with deep flows, that have been observed at these periods previously in both the Gulf Stream (e.g. Shay et al., 1995) and the Kuroshio extension (Greene et al., 2012). It should be noted that while the coherences between surface and deeper layers are statistically significant at periods shorter than ~30 days, the coherence values themselves are not as large as are observed at longer periods (typically < 0.6), and the spectra suggest that there is less energy at these time scales.

Stepping to a lower layer, the coherence between the main thermocline (at 500 dbar) and the upper and lower water column is similarly poor/insignificant except at periods shorter than about 50 days (Fig. 10). Flow within the main thermocline depth range itself is highly coherent, with values exceeding 0.9 between 250 and 750 dbar at periods as long as 100 days for zonal and meridional velocity as well as total speed. As with the surface meridional flow, there is a broad band of high coherence at about 30–50 days extending into the deep ocean (Fig. 10, top-middle panel) associated with a band of high energy in the variance preserving spectra of meridional velocity (Fig. 10, lower middle panel). In the zonal velocity there is a narrower band of coherence at about 30–35 days that also reaches quite deep, but in general the coherence of the zonal velocity is weaker than that of the meridional velocity, even for the longer time scales where there is significantly more energy in the zonal flows (periods greater than 50 days – compare Fig. 10 lower left and lower middle panels). The total speed

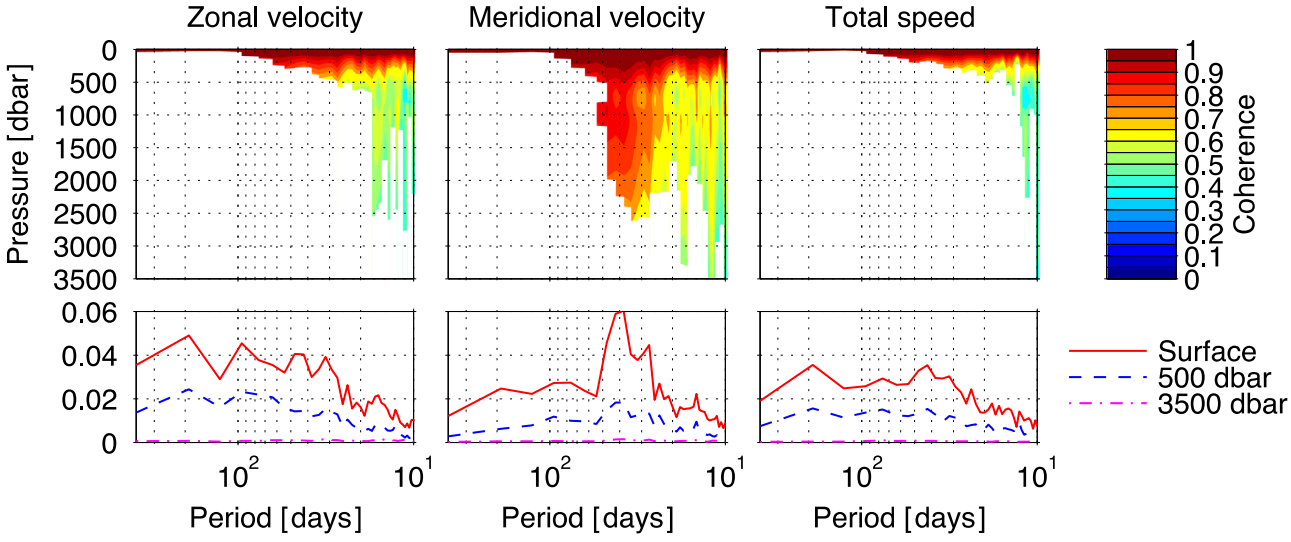

Fig. 9. *Top panels: Vertical coherence amplitude squared of velocity as a function of pressure and period for data from the SYNOP experiment. Coherences for the zonal velocity component (left), meridional velocity component (middle) and total speed (right) are shown. Coherence is calculated between the surface and each pressure level using the PIES-GEM data from thirteen locations within the grid (the mapping points nearest the current meter moorings). Only values that are different from zero at the 95% significance level are plotted, given the observed number of degrees of freedom (e.g. Emery and Thomson, 2004; Meinen et al. 2009). Lower panels: Variance preserving spectra (units: $m^2\ s^{-2}$) are plotted for the surface, 500 dbar, and 3500 dbar; spectra are shown for the zonal velocity (left), meridional velocity (middle) and total speed (right).*

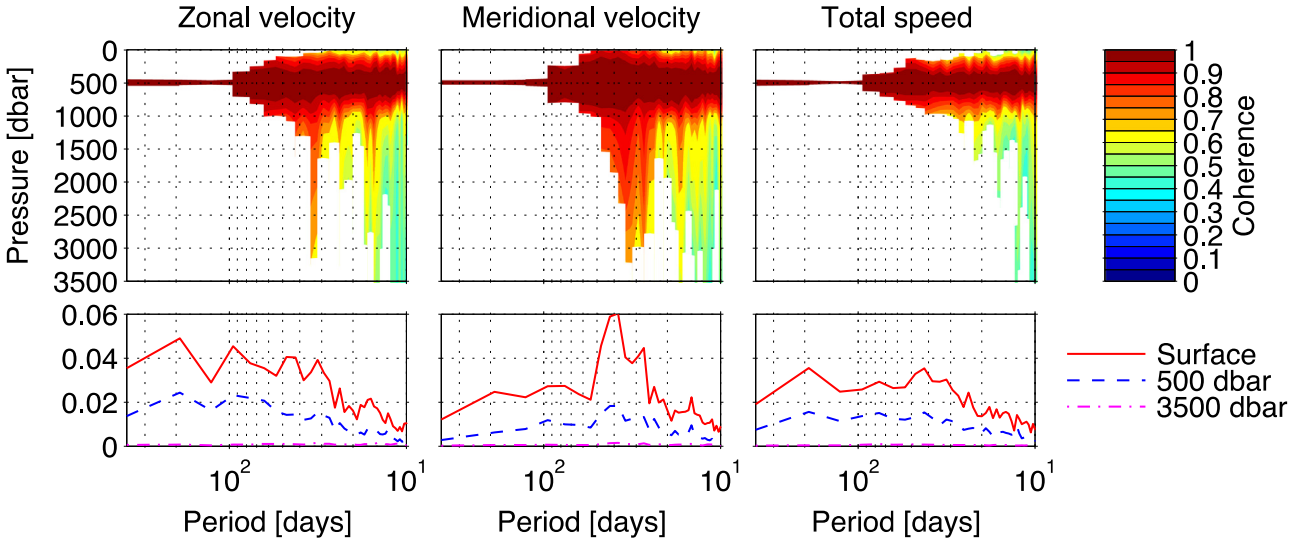

Fig. 10. *Same as Fig. 9 but for coherences calculated between the velocity at 500 dbar and other levels using the PIES-GEM data.*

exhibits little coherence into the deeper ocean at any time scale except below periods of ~20 days, where there is also little energy present in the spectra (Fig. 10, lower right panel).

Coherences between the deep (3500 dbar) flows and the rest of the water column (Fig. 11) show a consistent disconnection with the deep flows and the thermocline and surface flows. The 3500 dbar flows are highly coherent (>0.9) up to around 2000 dbar for time scales of 10–100 days, and significant coherence values are observed up to ~1000 dbar. The energy levels in the velocity spectra at 3500 dbar are fairly uniform/evenly-distributed across the same span of periods where the coherences are high (magenta dash-dot lines in Fig. 11, lower panels).

Before continuing, it is important to note that previous work has demonstrated event-based dynamical connections between Gulf Stream near-surface flows and the deep flows beneath the Gulf Stream all the way to the bottom. Savidge and Bane (1999a, 1999b), for example, looked at baroclinic-instability-based connections between steep meanders and deep cyclones, and it is clear that during these events there are three-dimensional motions that are connecting the flows in the deep and shallow layers. The key issue to understand for the results presented herein, however, is that these events are of limited duration and the deep features can initially horizontally propagate independently of the Gulf Stream meanders above until the features lock together (e.g. see Fig. 12 of Watts et al. (1995)). As such, looking in a time series correlation and/or coherence sense these limited length events will not indicate a significant coherence determined over the record length because the related variability was limited to only a short period of time (and with horizontally varying phases until 'locking' occurs between the shallow and deep flows). So the results presented here in no way argue that there are flaws in the mechanisms such as that described by Savidge and Bane (1999a, 1999b). What the results presented here do indicate is that those mechanisms are sufficiently irregular in time that they do not impact the overall time series coherence between layers, and that knowledge of the flow in the surface of the Gulf Stream does not predict the flow in deeper layers.

These results also suggest that, at least when determined in Eulerian coordinates, the variability of the Gulf Stream in the Mid-Atlantic Bight appears to be organized in three fairly independent layers with little coherence between the layers at periods longer than a few tens of days. This somewhat discouraging result (due to its negative implications for establishing observational proxies) immediately begs the question as to whether this lack of

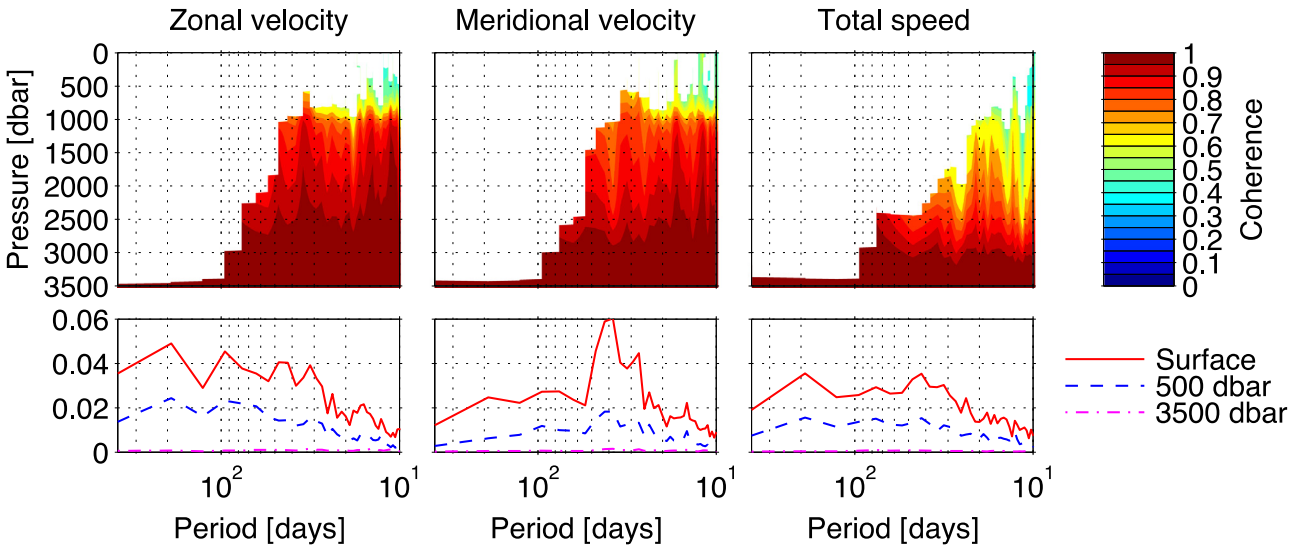

Fig. 11. *Same as Fig. 9 but for coherences calculated between the velocity at 3500 dbar and other levels using the PIES-GEM data.*

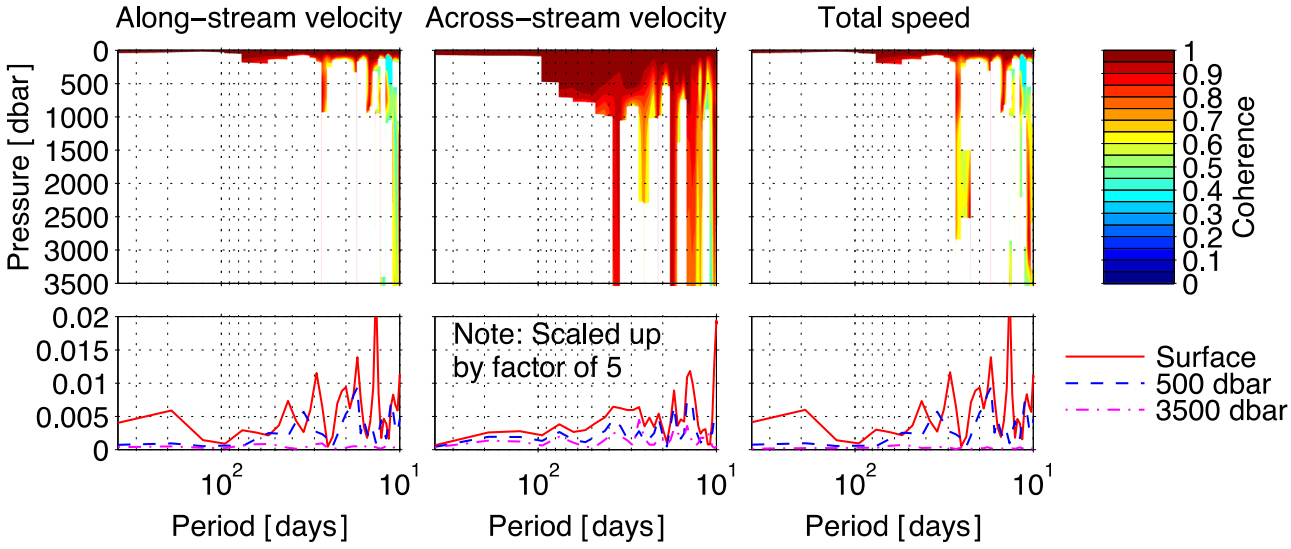

Fig. 12. *Coherence of surface currents with currents from other pressure levels (top panels) and selected variance preserving spectra (bottom panels), as in Fig. 9, but using currents referenced to stream coordinates (see the text) near the core of the Gulf Stream in the SYNOP region rather than the Eulerian data. Data from within ± 25 km of the core are used. Note that the variance preserving spectra for the across-stream component of the velocity (lower middle panel) have been multiplied by a factor of 5 so that they can be plotted on a similar scale as the along-stream component and the total speed.*

statistically-significant coherence is due to the method by which it was calculated. It is possible that the superposition of multiple phenomena with different vertical structures (such as the aforementioned deep cyclones and barotropic oscillations) results in a weak overall vertical coherence between the different layers. It is therefore worth evaluating vertical coherence from a different point of view, that is, in a stream coordinates reference frame, which removes a large fraction of the variability in the currents due to the Gulf Stream's principal meandering that originates in the thermocline layer. This idea is addressed next.

3.3. *Vertical coherence of the flow in Stream Coordinates*

Calculated near the core of the Gulf Stream at 38°N, the coherences between the stream coordinates along-stream surface velocity and the flows at deeper levels (Fig. 12, top left) show a slight increase compared to the zonal Eulerian flow[5] in the upper ~100 m (Fig. 9, top left). However, the significant coherences cover a smaller depth range for all time scales shorter than ~80 days. The across-stream component of the surface flow appears to have a higher coherence down to 500 dbar (Fig. 12, top middle, versus Fig. 9, top middle). However, the energy spectra of the across-stream flows (Fig. 12, bottom middle) are much weaker than the spectra of the along-stream flows. (N.b., because the magnitudes of the across-stream currents are much smaller than the magnitudes of the along-stream currents, the spectra of the across-stream flows were multiplied by a factor of five so that they could be meaningfully displayed on comparable axes in Fig. 12, lower panels.) There are a few narrow bands of high coherence, such as around periods of 15, 25 and 35 days depending on the component, possibly associated with the propagation of large scale, shorter period, modes of variability of the Gulf Stream (e.g. Robinson et al., 1974; Watts and Johns, 1982; Halliwell and Mooers, 1983; Teague and Hallock, 1990; Savidge, 2004). Many (but not all) of these bands of coherence correspond approximately to peaks in the energy spectra (Fig. 12, lower panels). But, overall there is still little significant coherence between the surface flows and those at depth. Note that the spectra of the stream coordinates currents are weaker than the Eulerian equivalents, since transformation to the stream coordinates reference frame removes a great deal of the energy associated with the principal meandering of the current.

As for the stream-coordinates surface currents, coherence between stream-coordinates currents in the main thermocline and other levels (Fig. 13) shows similar narrow bands of high coherence around 15, 25, 35 and 45 days depending on the component, with statistically insignificant coherence elsewhere. The coherence values within the main thermocline depth range are slightly higher (>0.95) than are found for the Eulerian zonal flows (Fig. 10). However, the vertical extent of the statistically significant coherences is somewhat smaller, except in the aforementioned narrow frequency bands. The across-stream component shows stronger vertical coherence, but again note that the energy levels in this component are weak, and the spectra had to be multiplied by five to plot them on axes consistent with the other components.

The deep (3500 dbar) stream coordinates velocities show high coherence throughout the layer below the main thermocline depth range (below roughly 1000 dbar), noticeably higher than the equivalent Eulerian coherences (compare Fig. 14 with Fig. 11). But there is little significant coherence with the thermocline or surface depth ranges (Fig. 14) except in the previously identified tight period bands around 15, 25, 35 and 45 days, depending on the component. While the coherence values for stream coordinates currents are higher throughout much of the deep ocean (>0.95), the vertical extent of statistically significant coherences is nearly the same as for the equivalent Eulerian currents (compare Figs. 14 and 11).

While transforming the Eulerian currents into stream coordinates does not remove the presence of external signals (e.g., persistent deep cyclones), it should provide a clearer quantification of the variability associated with flow along the baroclinic front. The similarity of the vertical coherences based on both stream coordinates and Eulerian currents suggests that there is little coherence in general between Gulf Stream velocity variability in the surface, thermocline, and deep layers near 38°N for variations with periods of 10 to 365 days.

[5] While highly variable, the time-mean Gulf Stream flow direction in this region is less than 20° from eastward, so the zonal component of the flow is the better Eulerian term for comparison with the along-stream flow in stream coordinates.

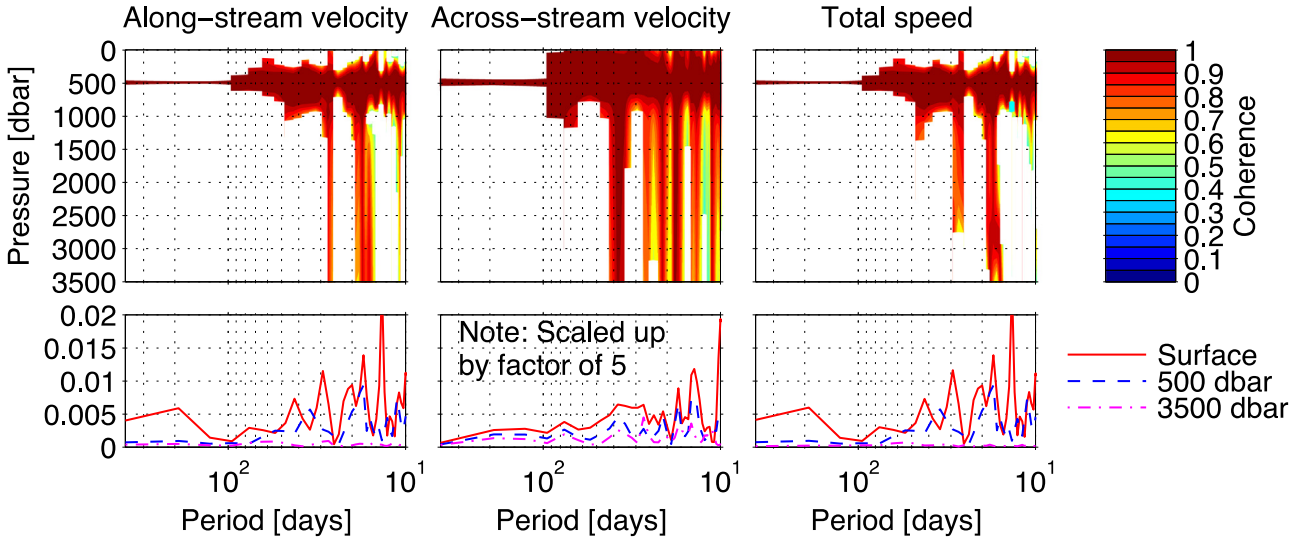

Fig. 13. *Same as Fig. 12, but for coherences between the stream coordinates currents at the 500 dbar level versus stream coordinates currents at other pressure levels.*

3.4. Vertical coherence of the flow at 42°N and 27°N

The lack of vertical coherence in the Gulf Stream at 38°N may reasonably be interpreted as a result of the current being in a freely-meandering state in a basin that experiences many other strong modes of variability that are not necessarily associated with the Gulf Stream flow at that location, such as topographic Rossby waves (e.g. Pickart, 1995) and deep cyclones (e.g. Savidge and Bane, 1999a, 1999b). If such is the case, then study of the Gulf Stream in either the downstream location where it has reattached to the shelf and become topographically controlled at 42°N or upstream where it is relatively shallow and is flowing through a narrow channel at 27°N may provide different results. As mentioned earlier, the NAC and Florida Straits data sets are not as optimal for determining the vertical coherence as they either provide only one component of the velocity (NAC) or are based on snapshot measurements (Florida Straits). Nevertheless, these data are useful for evaluating aspects of vertical coherence or correlation, respectively.

At 42°N the coherences (Fig. 15) are in general slightly higher than those observed at 38°N, and the bounds of the statistically significant coherences generally encompass a larger fraction of the full water column. The coherence values suggest more co-variability in the surface and thermocline depth layers; however, as at 38°N, they still suggest that there is not a high degree of coherence between the upper water column and deep flows in the North Atlantic Current at the observed periods. Coherences determined using the current meter data in the NAC region (not shown) are similar. This suggests that the variability of the flow at 42°N is organized in two fairly independent layers, with an upper ocean and deep ocean separated at 1000–1500 dbar, while at 38°N the flow variability appears to be organized in three nearly independent layers: near-surface (upper 200–300 dbar), thermocline (~250–750 dbar) and deep (1000+dbar).

At 27°N, the CTD/LADCP data cannot be used to calculate true frequency-dependent coherence functions, as the 55 sections are snapshot observations distributed irregularly in time. However, correlations between the velocities observed at the surface and the lower depths can be determined from the profile data (Fig. 16). Correlations were determined for each of the nine standard sites spanning the Florida Straits. Only at the very shallow (120 m deep) west side of the Straits is the correlation between surface and bottom velocity statistically significant at the 95% confidence level; at the other sites the correlations between the surface and the

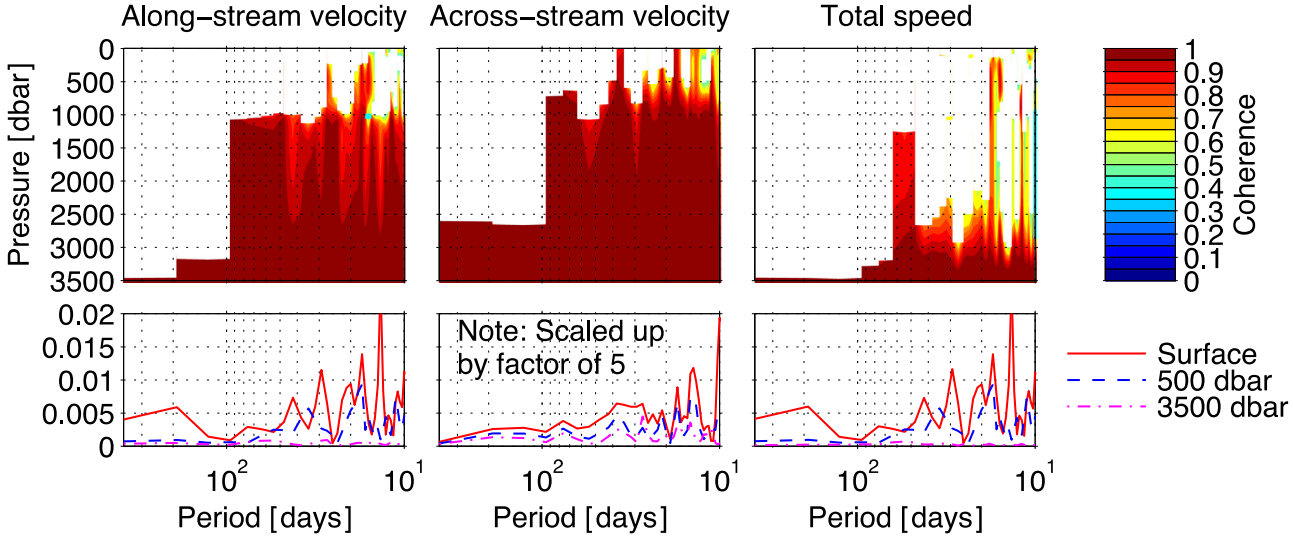

Fig. 14. *Same as Fig. 12, but for coherences between the stream coordinates currents at the 3500 dbar level versus stream coordinates currents at other pressure levels.*

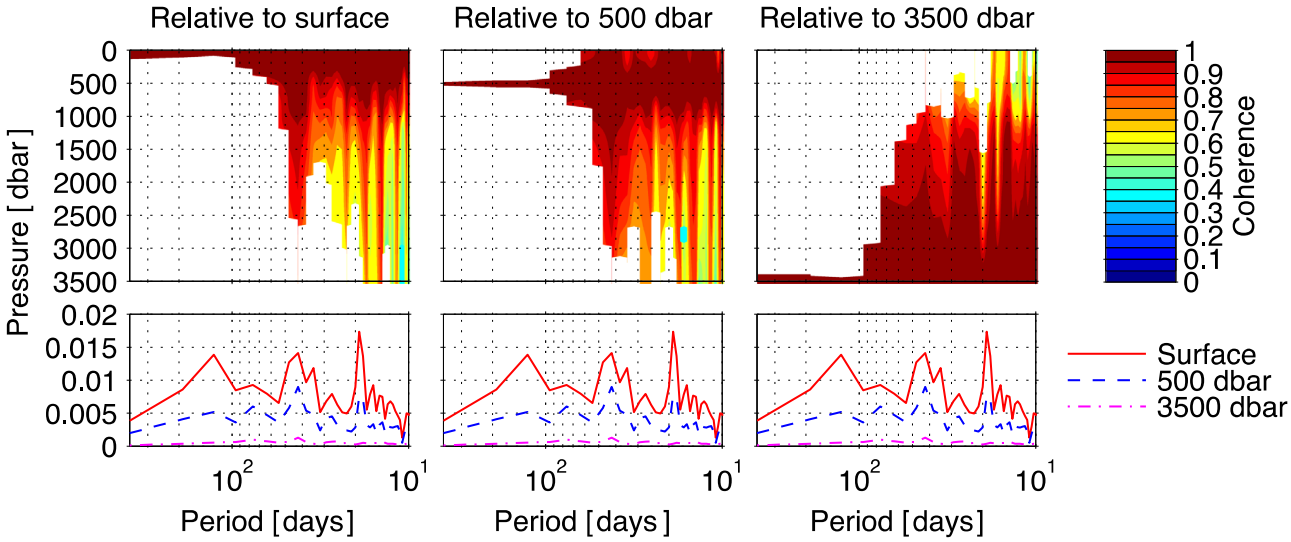

Fig. 15. *Vertical coherence amplitude squared of the absolute velocity observed in the NAC experiment. N.b., the NAC array only measured the component of the geostrophic velocity perpendicular to the line of instruments, i.e. the component of the flow oriented roughly 21° clockwise of true north. Coherences are calculated relative to the surface (left), 500 dbar (middle), and 3500 dbar (right) levels. Only values that are different from zero at the 95% significance level are plotted, given the observed number of degrees of freedom (e.g. Emery and Thomson, 2004; Meinen et al. 2009). Lower panels: Variance preserving spectra (units: $m^2\,s^{-2}$) are plotted for the surface, 500 dbar, and 3500 dbar. Note that all lower panels are identical – they are repeated to simplify comparison with the coherence panels.*

deeper levels are not statistically significant from zero below 200–400 dbar. Reanalysis of the data from ~60 Pegasus sections collected in the early 1980s (e.g. Leaman et al., 1987) finds similar low correlations between the near surface (~20 dbar) and near-bottom flows (not shown). Furthermore, calculating correlations using a few of the short (< 6 month) hourly current meter records for moorings that did not experience significant mooring motion (pressure changes < 20 dbar) during STACS (e.g. Lee and Williams, 1988) indicates that the current meters also find no significant correlation (generally $r < 0.2$) between the surface and the near bottom meridional velocities. This suggests that even in the tightly confined Florida Straits where the Florida Current/Gulf Stream is generally thought to fill the entire channel (e.g. Szuts and Meinen, 2013; Garcia and Meinen, 2014; see also Fig. 6 herein) there is no correlation between the surface and deep flows when integrating the coherence over a broad range of frequencies.

3.5. Downstream evolution of Gulf Stream transport

In addition to evaluating the vertical coherence of the velocity structure in the Gulf Stream at three locations, this reanalysis together with the results of previous studies motivates an evaluation of the downstream change in volume transport from 27°N to 42°N. Based on a host of observations of different types over the past few decades, it has been shown that the Gulf Stream transport increases from around 32 Sv in the Florida Straits (e.g., Larsen and Sanford, 1985; Meinen et al., 2010; and also from the newly analyzed CTD/LADCP sections used for Figs 4–6) to about 65–94 Sv as it approaches Cape Hatteras and then leaves the coast (e.g., Knauss, 1969; Leaman et al., 1989), and then ramps up to a maximum of nearly 150 Sv by 60°W, after which it remains essentially constant until east of 55°W where the recirculation cells begin to draw water out of the current (Hogg, 1992). By the time the Gulf Stream reaches 50°W the transport has dropped to about 120 Sv (Clarke et al., 1980). After this point the current loses some flow into the eastward flowing Azores Current, but the majority of the Gulf Stream waters turn northward to form the North Atlantic Current (Clarke et al., 1980). At this location (near 42°N), the NAC is a strong, coherent boundary current bounded on the offshore side by the powerful Mann Eddy. The net northward transport, including both the NAC and the inshore edge of the Mann Eddy, is roughly 146 Sv (Meinen and Watts, 2000; Meinen, 2001). The NAC then flows through a series of topographically-controlled stationary meanders, losing transport to the east as it flows northward along the eastern coast of Canada (Rossby, 1996).

These observations come from different years and even different decades, so the impact of long-period variability on the various transport estimates must be considered. Data spanning and/or separated by a decade or two is not available at most locations where Gulf Stream transport has been estimated. At those locations where it is available, such as in the Mid-Atlantic Bight (e.g., Rossby et al., 2010) and at the Southeast Newfoundland Ridge (e.g., Schott et al., 2004), there is little indication of long-period variations in the structure and transport of the Gulf Stream. In the Florida Straits at 27°N, the long, nearly-continuous estimates of transport from cable voltages and repeated sections of direct current observations (e.g. Meinen et al., 2010) have shown that while the Gulf Stream at that location experiences very large fluctuations at periods of days to months, low-frequency variations are quite weak. Evaluation of the 30+year record of voltage-based transport estimates[6] from cables spanning the Straits indicates that the largest difference between any individual annual mean transport value and the long-term mean value of 32 Sv is less than 5%. (N.b., the lack of variability in the transport and structure of the Gulf Stream does not imply that there have been no long-period changes in the location of its path, which is a quite different issue that is not addressed here.)

Fig. 17 illustrates the available estimates of the Gulf Stream transport along its path from the Florida Straits to the beginning of the North Atlantic Current. All of these estimates, with the exception of the Knauss (1969) estimates, are based on time-series averages (Clarke et al., 1980; Hogg, 1992; Johns et al., 1995; Meinen, 2001; Meinen et al., 2010) or are the average of a large number of sections (Leaman et al., 1989). The Knauss (1969) values are averages of only two sections at each of two locations. The new data presented herein for 27°N produce transport estimates very close (within < 1 Sv) to the historical estimates at the same latitude. Using only these admittedly sparse observations, and

[6] The transport data are available from www.aoml.noaa.gov/phod/floridacurrent/.

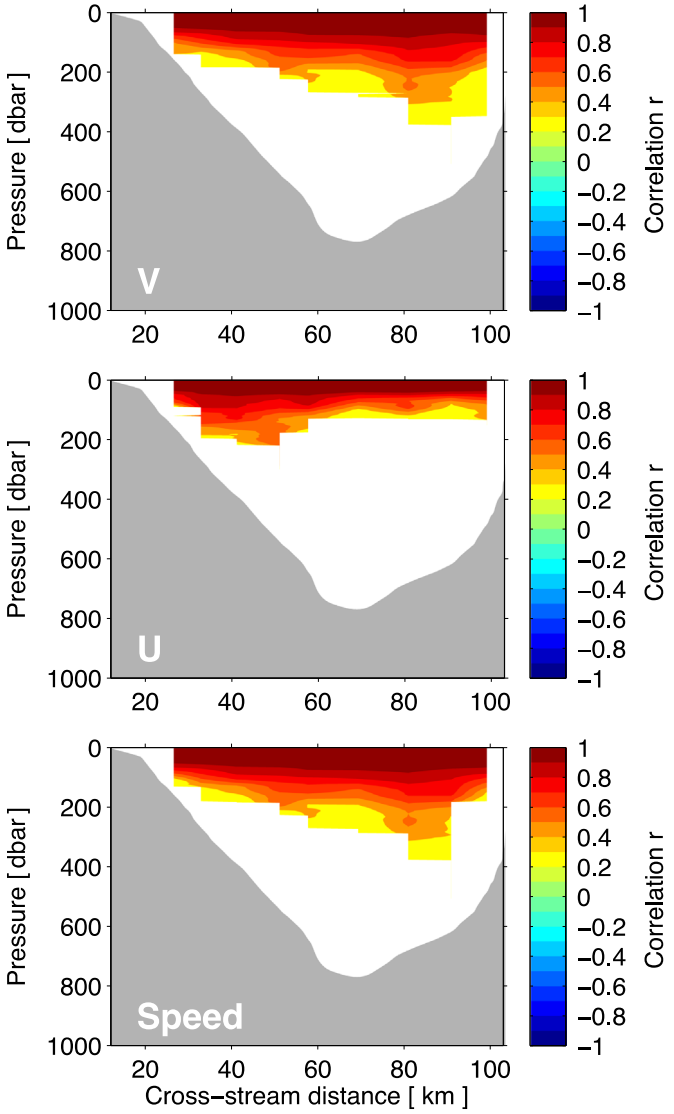

Fig. 16. *Correlation between surface velocity from the LADCP casts in the Straits of Florida and the velocity at other depths. The top, middle, and bottom panels show data respectively for meridional velocity, zonal velocity, and total speed. Only correlations that exceed the 95% confidence limits are plotted. Gray shading indicates the ocean bottom.*

neglecting the Knauss (1969) results that were based on limited data, the rate of inflow into the Gulf Stream is fairly constant from the Florida Straits up until 60°W at 3–4 Sv per 100 km. The inflow rate from 73°W to 68°W is about 20% higher (4.4 Sv per 100 km rather than 3.6 Sv per 100 km), after which the rate remains essentially constant between 68°W and 60°W (Fig. 17b and c). The rate of outflow between 55°W and 50°W (8.1 Sv per 100 km) is 50–100% larger than the peak inflow rates elsewhere along the path (again neglecting the Knauss (1969), values). The inflow rate into the developing North Atlantic Current between 50°W and 46°W is nearly 40% larger than the inflow rates into the Gulf Stream to the west, demonstrating the strength of the Mann Eddy and other recirculations associated with the higher latitude portion of the gyre (e.g. Rossby, 1996; Meinen, 2001).

The bulk inflow/outflow numbers presented above suggest that the changes in the Gulf Stream's transport are fairly uniform along its path. However, stream coordinates mean cross-stream flows

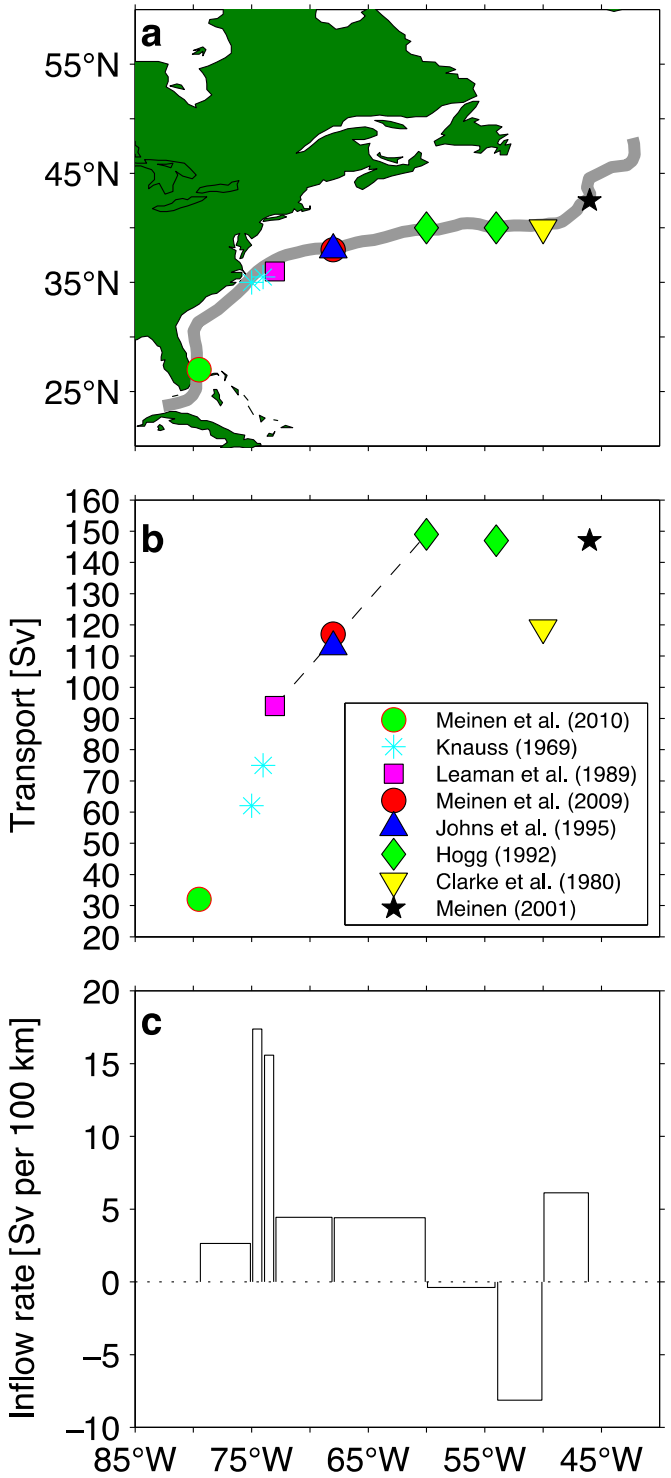

Fig. 17. *Downstream changes in transport along the Gulf Stream path as determined by various historical studies. The Knauss (1969) study represented the average of only two sections per longitude; all other studies represent multi-year time-mean transports of repeated sections (Leaman et al., 1989), submarine cable (Meinen et al., 2010), or mooring observations. The transports calculated from the new data presented herein at 27°N agree well (within ~1 Sv) with the historical estimate shown in the figure. (a) Map of the study locations, with an idealized Gulf Stream path (gray line). The mean SST front location of Lee and Cornillon (1996) was used between Cape Hatteras and 50 °W in creating the Gulf Stream path. (b) Mean transports from the indicated studies. The dashed line connects the observations immediately west and east of the SYNOP Central Array. (c) Inflow/outflow rates between observations shown in panel (b) using distances along the approximate Gulf Stream path shown in panel (a).*

estimated at 68°W (Meinen et al., 2009) suggest that the inflow there is much higher than the bulk estimate of ~4 Sv per 100 km in Fig. 17c. The vertical mean cross-stream velocities presented by Meinen et al. (2009) have peak inflow values of 2–3 cm/s at roughly 100 km on either side of the front. These values are only marginally different from zero at a one standard error level and are not significantly different from zero at 95% confidence. Nevertheless, given a rough mean depth of 4500 m, the inflow, if real, would translate into a convergence of about 18–27 Sv per 100 km, which is a bit larger than but not inconsistent with the Johns et al. (1995) estimate of inflow at this longitude from the SYNOP moored current meter data (12 Sv per 100 km, including only the inflow from the north side). These values of 18–27 Sv per 100 km are a factor of about five to six times larger than the bulk value of ~4 Sv per 100 km found between 73°W and 55°W. If real, such a large inflow would suggest that 68°W may be a location of peak inflow for the recirculation gyres on either side of the current, as suggested by Johns et al. (1995), perhaps as the result of a local (zonally narrow) amplification of the recirculation associated with the semi-permanent meander found at 68°W (Watts et al., 1995).

4. Discussion and conclusions

Consistent reanalysis of observations of the Gulf Stream at three locations along its path, 27°N, 38°N, and 42°N, has produced standardized depictions of the time mean structure and flow at locations where the Gulf Stream is confined within a channel, where it is a freely-meandering jet, and where it is flowing along the continental slope. The inflow and outflow estimates associated with these and other historical Gulf Stream studies continue to support a picture of along-stream varying inflow from Florida to 60°W with maximum inflow just east of Cape Hatteras and around 68°W, and large outflow and inflow on the west and east sides of the Newfoundland Ridge, respectively.

Perhaps the most important result of this study derives from the analysis of the vertical coherence of the variability of the Gulf Stream flow. At all three locations, the time-mean flow at all depths has a significant component of the flow in the same direction (see Fig. 6). However, the time-varying flows tell a very different story. Calculated either in Eulerian or Stream coordinates, the data indicate that the variability of the Gulf Stream flow at the surface is generally uncorrelated with the flow variations within the main thermocline depths and/or within the deep ocean at all three locations studied here (27°N, 38°N, and 42°N). Detailed analyses at 38°N and 42°N suggest that the lack of coherence at those locations is observed at essentially all time scales (with a few exceptions) between a few days and a year (which is the longest period that could be studied with these data sets). This does not suggest that there is *never* correlated variations in the upper water column and at depth – as noted earlier there have been several studies documenting event-based dynamical interactions between upper and deep layer flows – however in a time series sense this suggests that the surface flows are not a reliable predictor of flows at deeper levels. The implications of these results are both important for future observational efforts and a bit daunting for schemes to create simple proxies for the temporal variation of the Gulf Stream flow. These results suggest that observing only a portion of the Gulf Stream flow (such as only the upper 1000 m) and attempting to 'fill' the missing deep flow, for instance with any sort of climatological extrapolation, will not result in accurate velocities or transports (a concern also expressed by Rossby et al. (2010)), since the deep flow at the time of observation would be uncorrelated with the observed upper water column flow.

Furthermore, the lack of vertical coherence has serious negative implications for the application of remote observation methodologies that attempt to determine proxies, such as from time-varying altimetry sea-surface height (SSH) gradients, for the Gulf Stream's time-dependent flow. At best, this method may yield accurate flow estimates from the surface through the thermocline, while misrepresenting the deep flow. At worst, it would not even represent well the flow in the thermocline.

To properly measure and characterize the full depth velocity structure and transport of the Gulf Stream, therefore, it is necessary to measure the flow at all depths. This can be done indirectly (using PIES along with the hydrographic-derived shear profiles from the GEM methodology), or directly (with tall current meter moorings or dynamic height moorings coupled with bottom pressure recorders), but measurements of only one layer (e.g. via hull-mounted ADCP or via altimetry) will not produce the accurate estimates of the time-varying full-depth flow that are likely necessary for understanding the long-time-scale variability of the Gulf Stream system and its interaction with other elements of the global hydrosphere. It should be noted that this does not mean that the Gulf Stream is not a vertically connected jet in a dynamical sense – of course it is. The implication is that the ocean is extraordinarily variable, with eddies and other features acting on geostrophic spatial scales independently at all depths at times, even at the surface. So to truly measure and understand ocean flows, we need to observe all depths simultaneously, not just a portion of the water column.

Acknowledgements

Rigoberto Garcia helped with some of the 68°W and Straits of Florida calculations. Randy Watts and Karen Tracey provided help with many earlier calculations for the North Atlantic Current, and were invaluable resources in providing the optimally mapped travel time and pressure data sets from the SYNOP Central Array. Libby Johns, Molly Baringer, Bill Johns and Bob Molinari provided several helpful suggestions during the early stages of preparing this manuscript, and the anonymous reviewers made many helpful suggestions for improving the paper. CM was supported in this work by the NOAA Climate Program Office-Climate Observation Division (via the Western Boundary Time Series project) and the NOAA Atlantic Oceanographic and Meteorological Laboratory. At U. Hawaii, the work was supported by NSF Grant OCE03-52229.

Appendix:

Because the GEM analysis technique for IES data provides time series of temperature (or salinity, or density) at different pressure levels using a single time series of travel time (Meinen and Watts, 2000; Watts et al., 2001a, 2001b), it is often suggested that the variability in temperature, salinity, and geostrophically-derived velocity at different pressure levels determined from the IES+GEM technique must be perfectly correlated with one another. This is not in practice true, for several reasons. First, in terms of the temperature and salinity, this assertion is false because it neglects the input of the GEM fields themselves, which are derived from completely independent hydrographic data (e.g. Meinen and Watts, 2000). Essentially, a GEM field is purely empirical; there is no reason to expect that the isotherms will be parallel to one another. Consider the temperature GEM field for the NAC region, in particular the temperature values at 100 and 700 dbar (extracted from Fig. 2 and plotted as Fig. A1). When an IES measures a travel time change from 2.62 s to 2.63 s, for example, the estimated temperature at 100 dbar will increase while the estimated

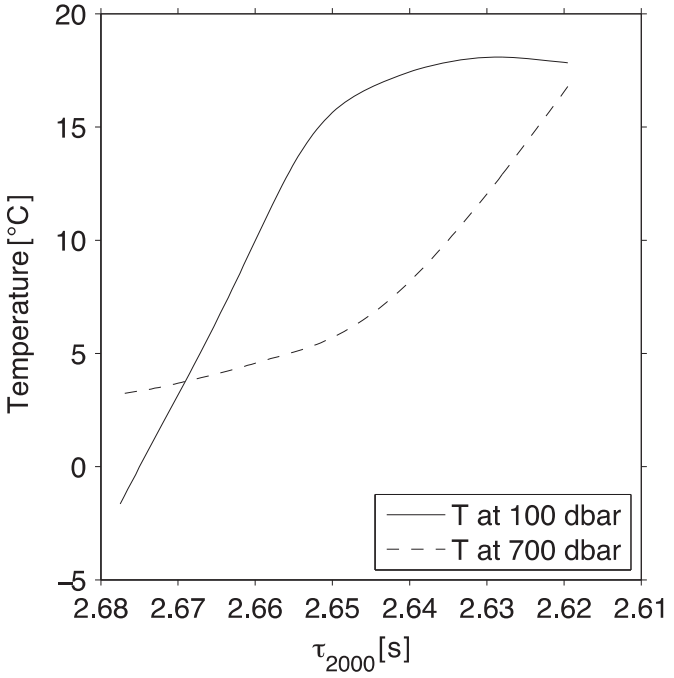

Fig. A1. *Temperature at two pressure levels as a function of acoustic travel time extracted from the temperature GEM field (Fig. 2).*

temperature at 700 dbar will decrease. If at a later point in time the same IES measures a travel time change from 2.65 to 2.66 s, the estimated temperatures at both 100 and 700 dbar will decrease. Thus, a single IES travel time record can provide independent, non-correlated, variability at two depths above the instrument through the combination with the independent hydrography-derived GEM fields.

Moreover, the geostrophic relative velocity estimates that come from a pair of IES moorings require, in fact, two moorings. Depending on the distance between the moorings, as compared to the horizontal correlation length scale, these two sites can represent completely independent or partially independent sources of information. Furthermore, the absolute velocities discussed herein are based on PIES, which means that in addition to two travel time records, there are also two pressure records, which are fully independent of the travel time records and may be independent of one another as well, again depending on the horizontal instrument spacing relative to the correlation length scale. So each absolute velocity profile between a pair of PIES is based on at least two completely independent time series, possibly four depending on the horizontal spacing, plus the (also independent) variability inherent in the GEM field. So while the PIES-GEM technique is not perfect, and it does involve some averaging that will reduce some of the high-mode variability, the PIES-GEM technique can conceptually capture several independent modes of variability.

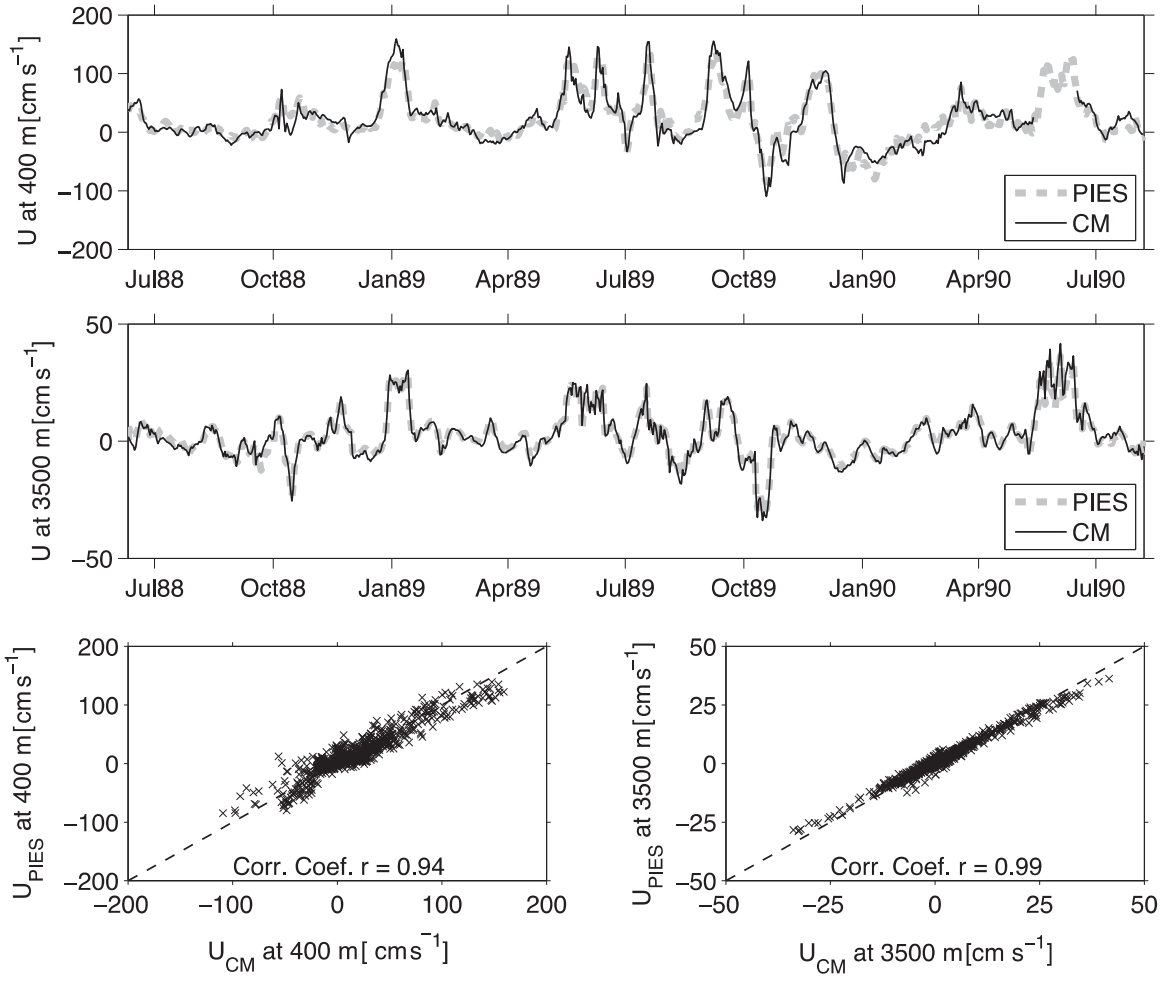

Fig. A2. *Comparison of mooring-motion-corrected current meter zonal velocity observations at Site I5 in the SYNOP Central Array to the PIES-GEM estimated zonal velocity at that same site. Time series comparisons are shown for the nominal depth of 400 m (panel a) and at 3500 m (panel b). The time series are also plotted against one another to illustrate the high correlation for the 400 m records (panel c) and for the 3500 m records (panel d); the correlation coefficients are indicated on panels c and d. Note that the correlation between the current meter measured velocity at the 400 m and 3500 m depths is much lower (r=0.59; compare black lines in panels a and b) than the correlation between current meter and PIES velocity at one depth (r=0.94 at 400 m; r=0.99 at 3500 m). For the PIES the correlation between estimated velocity at 400 m and 3500 m is also much lower (r=0.69; compare gray dashed lines in panels a and b).*

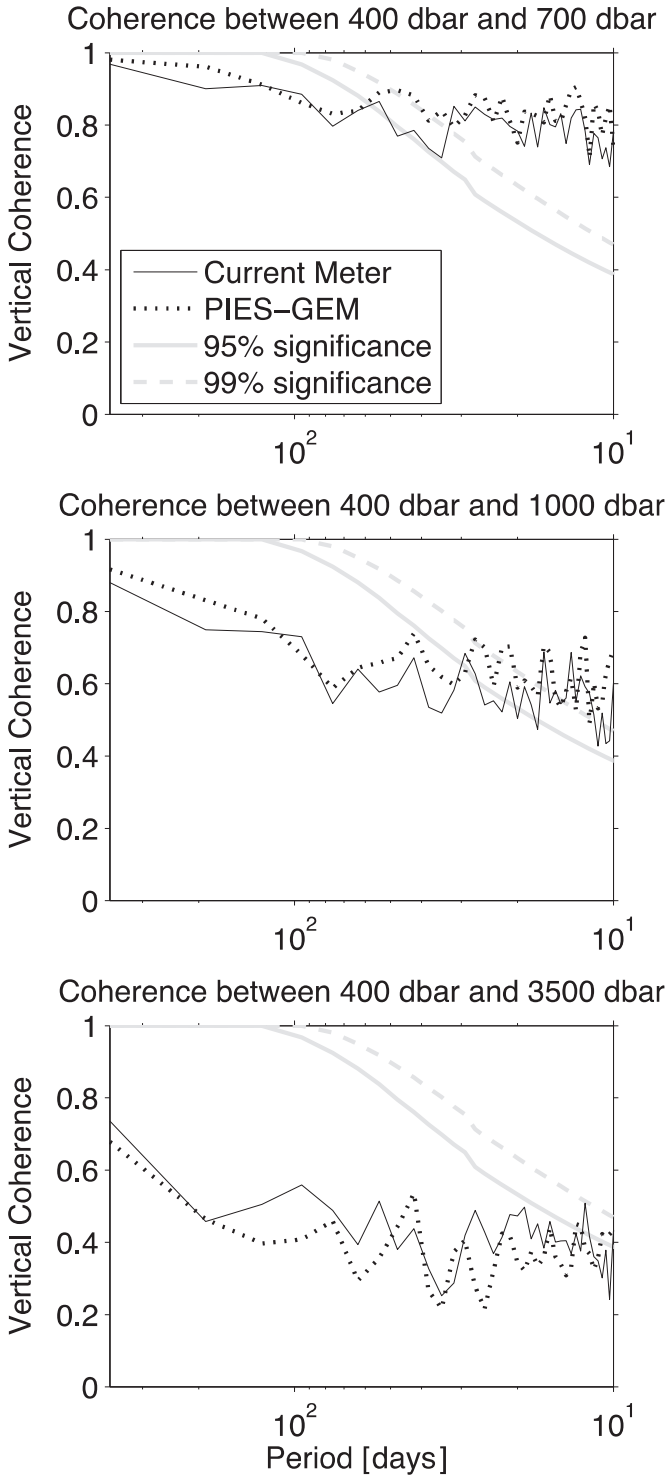

Fig. A3. *Comparison of the vertical coherence between flow speeds at selected levels from current meter data and from PIES-GEM data. Coherences were calculated between the indicated levels from each of the mooring motion corrected current meter time series produced by Cronin and Watts (1996) and the results were averaged to produce the solid lines in this figure. The PIES-GEM data at each of the current meter mooring sites were used to calculate vertical coherence between the same levels and the results were averaged to produce the dotted lines shown. Significance levels are indicated following Thompson (1979).*

The similar abilities of the PIES-GEM technique and the more traditional current meter mooring to capture uncorrelated/incoherent variability at different depths can be illustrated by plotting side-by-side time series and/or by plotting time series against one another (Fig. A2). The zonal velocity at Site I5 in the SYNOP Central Array at two depths, 400 m and 3500 m, demonstrate both correlated and uncorrelated variability (compare Fig. A2a and A2b: overall correlation between current meter velocities at these two depths is not high, r=0.59; the correlation between velocities at the same depths from PIES-GEM is also modest, r=0.69). Given the independent variations at the two depths, the fact that the PIES-GEM estimated velocities correlate so highly with the current meter velocity at each depth (r=0.94 at 400 m; r=0.99 at 3500 m) illustrates the ability of the PIES-GEM to capture independent variability at different depths. To further test whether the PIES-GEM velocity data can be used to evaluate vertical coherence of velocity, a comparison was made between the vertical coherence estimated by the PIES at 13 sites in the SYNOP array at 38 °N to the vertical coherence calculated using the mooring motion corrected velocities from the coincident current meter data (Cronin and Watts, 1996) at the same 13 sites (Fig. A3). While the precise details of the coherence between the three pairs of pressure levels are not identical, which is not surprising as the current meter measurements are true point measurements in the horizontal while the PIES-GEM velocities are true horizontal averages over the roughly 40 km distance between PIES sites, the level of coherence between flows at each pair of depths is very similar. This suggests that the coherence results from the current meter moorings are consistent with those from the PIES-GEM velocities.

References

Bower, A.S., Hogg, N.G., 1996. Structure of the Gulf Stream and its recirculations at 55ºW. J. Phys. Oceangr. 26 (6), 1002–1022.

Bower, A.S., Rossby, H.T., Lillibridge, J.L., 1985. The Gulf Stream—barrier or blender? J. Phys. Oceangr. 15 (1), 24–32.

Clarke, R.A., Hill, H.W., Reiniger, R.F., Warren, B.A., 1980. Current system South and East of the grand banks of Newfoundland. J. Phys. Oceangr. 10 (1), 25–65.

Cronin, M., Watts, D.R., 1996. Eddy-Mean flow interaction in the Gulf Stream at 68ºW. Part I: eddy energetics. J. Phys. Oceangr. 26 (10), 2107–2131.

Donohue, K.A., Watts, D.R., Tracey, K.L., Greene, A.D., Kennelly, M., 2010. Mapping circulation in the Kuroshio extension with an array of current and pressure recording inverted echo sounders. J. Atmos. Oceanogr. Technol. 27 (3), 507–527. http://dx.doi.org/10.1175/2009JTECHO686.1.

Ebbesmeyer, C.C., Lindstrom, E.J., 1986. Structure and origin of 18° water observed during the POLYMODE local dynamics experiment. J. Phys. Oceangr. 16, 443–453.

Emery, W.J., Thomson, R.E., 2004. Data Analysis Methods in Physical Oceanography. Elsevier, United States, p. 638.

Garcia, R.F., Meinen, C.S., 2014. Accuracy of Florida Current volume transport measurements at 27°N using multiple observational techniques. J. Atmos. Ocean. Technol. 31 (5), 1169–1180. http://dx.doi.org/10.1175/JTECH-D-13-00148.1.

Gill, A.E., 1982. Atmosphere-Ocean Dynamics. Academic Press, United States, p. 662.

Greene, A.D., Watts, D.R., Sutyrin, G.G., Sasaki, H., 2012. Evidence of vertical coupling between the Kuroshio extension and topographically controlled deep eddies. J. Mar. Res. 70, 719–747.

Halliwell Jr., G.R., Mooers, C.N.K., 1983. Meanders of Gulf Stream downstream from cape Hatteras 1975–1978. J. Phys. Oceanogr. 13, 1275–1292.

Hogg, N.G., 1992. On the transport of the Gulf Stream between Cape Hatteras and the grand banks. Deep Sea Res. 39, 1231–1246.

Hummon, J.M., Rossby, T., 1998. Spatial and temporal evolution of a Gulf Stream crest-warm core ring interaction. J. Geophys. Res. 103 (C2), 2795–2809.

Johns, E., Watts, D.R., Rossby, H.T., 1989. A test of geostrophy in the Gulf Stream. J. Geophys. Res. 94 (C3), 3211–3222.

Johns, W.E., Schott, F., 1987. Meandering and transport variations of the Florida Current. J. Phys. Oceanogr. 17 (8), 1128–1147.

Johns, W.E., Shay, T.J., Bane, J.M., Watts, D.R., 1995. Gulf Stream structure, transport, and recirculation near 68°W. J. Geophys. Res. 100 (C1), 817–838.

Joyce, T.M., 1984. Velocity and hydrographic structure of a Gulf Stream warm-core ring. J. Phys. Oceanogr. 14 (5), 936–947.

Joyce, T.M., Wunsch, C., Pierce, S.D., 1986. Synoptic Gulf Stream velocity profiles through simultaneous inversion of hydrographic and acoustic Doppler data. J. Geophys. Res. 91 (C6), 7573–7585.

Knauss, J.A., 1969. A note on the transport of the Gulf Stream. Deep Sea Res. 16 (Suppl.), S117–S123.

Larsen, J.C., Sanford, T.B., 1985. Florida current volume transports from voltage measurements. Science 227, 302–304.

Leaman, K.D., Molinari, R. L., Vertes, P.S., 1987. Structure and Variability of the Florida Current at 27ºN: April 1982–July 1984, vol. 17 (5), pp. 565–583.

Leaman, K.D., Johns, E., Rossby, T., 1989. The average distribution of volume

transport and potential vorticity with temperature at three sections across the Gulf Stream. J. Phys. Oceanogr. 19 (1), 36–50.
Lee, T., Cornillon, P., 1996. Propagation of Gulf Stream meanders between 74° and 70°W. J. Phys. Oceanogr. 26 (2), 205–224.
Lee, T.N., Schott, F.A., Zantopp, R., 1985. Florida current: low-frequency variability as observed with Moored Current meters during April 1982 to June 1983. Science 227, 298–302.
Lee, T.N., Williams, E., 1988. Wind-forced transport fluctuations of the Florida Current. J. Phys. Oceanogr. 18 (7), 937–946.
Logoutov, O., Sutyrin, G., Watts, D.R., 2001. Potential vorticity structure across the Gulf Stream: observations and a PV-Gradient model. J. Phys. Oceanogr. 31, 637–644.
Lozier, M.S., Owens, W.B., Curry, R.G., 1995. The climatology of the North Atlantic. Prog. Oceanogr. 36, 1–44.
Mann, C.R., 1967. The termination of the Gulf Stream and the beginning of the North Atlantic Current. Deep Sea Res. 14, 337–359.
McCarthy, G.D., Smeed, D.A., Johns, W.E., Frajka-Williams, E., Moat, B.I., Rayner, D., Baringer, M.O., Meinen, C.S., Bryden, H.L., 2015. Measuring the Atlantic meridional overturning circulation at 26°N. Prog. Oceanogr. 130, 91–111. http://dx.doi.org/10.1016/j.pocean.2014.10.006.
Meinen, C.S., Watts, D.R., 1998. Calibrating inverted echo sounders equipped with pressure sensors. J. Atmos. Ocean. Technol. 15 (6), 1339–1345.
Meinen, C.S., Watts, D.R., Allyn Clarke, R., 2000. Absolutely referenced geostrophic velocity and transport on a section across the North Atlantic Current. Deep Sea Res. 47, 309–322.
Meinen, C.S., Watts, D.R., 2000. Vertical structure and transport on a transect across the North Atlantic Current near 42°N: time series and mean. J. Geophys. Res. 105 (C9), 21869–21891.
Meinen, C.S., 2001. Structure of the North Atlantic Current in Stream-coordinates and the circulation in the Newfoundland basin. Deep Sea Res. I 48, 1553–1580.
Meinen, C.S., Luther, D.S., 2003. Comparison of methods of estimating mean synoptic current structure in "Stream Coordinates" reference frames with an example from the Antarctic Circumpolar Current. Deep Sea Res. I 50, 201–220.
Meinen, C.S., Luther, D.S., Baringer, M.O., 2009. Structure and transport of the Gulf Stream at 68ºW: revisiting older data sets with new techniques. Deep Sea Res. I 56 (1), 41–60. http://dx.doi.org/10.1016/j.dsr.2008.07.010.
Meinen, C.S., Baringer, M.O., Garcia, R.F., 2010. Florida current transport variability: an analysis of annual and longer-period signals. Deep Sea Res. I 57 (7), 835–846. http://dx.doi.org/10.1016/j.dsr.2010.04.001.
Molinari, R.L., Maul, G.A., Chew, F., Wilson, W.D., Bushnell, M., Mayer, D., Leaman, K., Schott, F., Lee, T., Zantopp, R., Larsen, J.C., Sanford, T.B., 1985a. Subtropical Atlantic climate studies: introduction. Science 227, 292–295.
Molinari, R.L., Wilson, W.D., Leaman, K., 1985b. Volume and heat transports of the Florida Current: april 1982 through August 1983. Science 227, 295–297.
Pickart, R.S., Watts, D.R., 1990. Deep western boundary current variability at Cape Hatteras. J. Mar. Res. 48, 765–791.
Pickart, R.S., 1995. Gulf Stream-generated topographic Rossby waves. J. Phys. Oceanogr. 25 (4), 574–586.
Robinson, A.R., Luyten, J.R., Fuglister, F.C., 1974. Transient Gulf Stream meandering. Part I: an observational experiment. J. Phys. Oceanogr. 4, 237–255.
Rossby, T., 1969. On monitoring depth variations of the main thermocline acoustically. J. Geophys. Res. 74 (23), 5542–5546.
Rossby, T., 1996. The North Atlantic Current and surrounding waters: at the crossroads. Rev. Geophys. 34 (4), 463–481.
Rossby, T., Benway, R.L., 2000. Slow variations in mean path of the Gulf Stream east of Cape Hatteras. Geophys. Res. Lett. 27 (1), 117–120.
Rossby, T., Flagg, C., Donohue, K., 2010. On the variability of Gulf Stream transport from seasonal to decadal timescales. J. Mar. Res. 68, 503–522.
Savidge, D.K., Bane Jr., J.M., 1999a. Cyclogenesis in the deep ocean beneath the Gulf Stream: 1. Description. J. Geophys. Res. 104 (C8), 18111–18126.
Savidge, D.K., Bane Jr., J.M., 1999b. Cyclogenesis in the deep ocean beneath the Gulf Stream: 2. Dynamics. J. Geophys. Res. 104 (C8), 18127–18140.
Savidge, D.K., 2004. Gulf Stream meander propagation past Cape Hatteras. J. Phys. Oceanogr. 34 (9), 2073–2085.
Schmeits, M.J., Dijkstra, H.A., 2000. Physics of the 9-month variability in the Sulf Stream region: combining data and dynamical systems analyses. J. Phys. Oceanogr. 30 (8), 1967–1987.
Schott, F.A., Zantopp, R., Stramma, L., Dengler, M., Fischer, J., Wibaux, M., 2004. Circulation and deep-water export at the western exit of the Subpolar North Atlantic. J. Phys. Oceanogr. 34 (4), 817–843.
Shay, T.J., Bane, J.M., Watts, D.R., Tracey, K.L., 1995. Gulf Stream flow field and events near 68°W. J. Geophys. Res. 100 (C11), 22565–22589.
Smeed, D.A., McCarthy, G., Cunningham, S.A., Frajka-Williams, E., Rayner, D., Johns, W.E., Meinen, C.S., Baringer, M.O., Moat, B.I., Duchez, A., Bryden, H.L., 2014. Observed decline of the Atlantic meridional overturning circulation 2004–2012. Ocean Sci. 10, 29–38. http://dx.doi.org/10.5194/os-10-29-2014.
Smith, W.H.F., Sandwell, D.T., 1997. Global sea floor topography from satellite altimetry and ship depth soundings. Science 277 (5334), 1956–1962.
Szuts, Z.B., Meinen, C., 2013. Salinity transport in the Florida Straits. J. Atmos. Ocean. Technol. 30, 971–983. http://dx.doi.org/10.1175/JTECH-D-12-00133.1.
Teague, W.J., Hallock, Z.R., 1990. Gulf Stream path analysis near the New England Seamounts. J. Geophys. Res. 95 (C2), 1647–1662.
Thompson, R.O.R.Y., 1979. Coherence significance levels. J. Atmos. Sci. 36 (10), 2020–2021.
Watts, D.R., Rossby, H.T., 1977. Measuring dynamic heights with inverted echo sounders: results from MODE. J. Phys. Oceanogr. 7, 345–358.
Watts, D., Johns, W.E., 1982. Gulf Stream meanders: observations on propagation and growth. J. Geophys. Res. 87 (C12), 9467–9476.
Watts, D.R., Tracey, K.L., Bane, J.M., Shay, T.J., 1995. Gulf Stream path and thermocline structure near 74°W and 68°W. J. Geophys. Res. 100 (C9), 18291–18312.
Watts, D.R., Qian, X., Tracey, K.L., 2001a. Mapping abyssal current and pressure fields under the meandering Gulf Stream. J. Atmos. Ocean. Technol. 18 (6), 1052–1067.
Watts, D.R., Sun, C., Rintoul, S., 2001b. A two-dimensional gravest empirical mode determined from hydrographic observations in the Subantarctic Front. J. Phys. Oceanogr. 31 (8), 2186–2209.
Worthington, L.V., 1959. The 18° water in the Sargasso Sea. Deep Sea Res. 5, 297–305.